UNIVERSITÀ
DEGLI STUDI
DI PADOVA

DIPARTIMENTO
DI INGEGNERIA
DELL'INFORMAZIONE

Ph.D. School in Information Engineering
Section: Bioengineering
Series: XXVII

DEVELOPMENT AND USE OF A NOVEL MODEL OF HEPATIC INSULIN EXTRACTION DURING AN ORAL TEST

School director
Prof. Matteo Bertocco

Bioengineering Coordinator
Prof. Giovanni Sparacino

Advisor
Prof. Chiara Dalla Man

Ph.D. Candidate
Francesca Piccinini

A thesis submitted for the degree of
Philosophiæ Doctor (PhD)
2015

Contents

Abstract

English

The regulation of glucose metabolism, in healthy subjects, is based on a complex control system which aims to maintain plasma glucose concentrations within a narrow range (70÷180 mg/dl). Insulin, a hormone secreted by pancreatic beta-cells, is fundamental in maintaining glucose homeostasis, by reducing liver glucose production, while promoting its utilization by the insulin-dependent organs. The inability of beta-cells to adequately secrete insulin creates metabolic disorders which can result in glucose intolerance and even diabetes mellitus. There are two different kinds of diabetes: type 1 diabetes (T1DM), characterized by a total inability of pancreatic beta-cells to secrete insulin, and type 2 diabetes (T2DM), in which, because of insulin resistance, tissues are unable to appropriately utilize glucose, and insulin secretion is unable to compensate for this defect. Given the increasing prevalence of diabetes, a complete understanding of all the mechanisms involved in the glucose regulation system is essential.

The liver is a fundamental organ in glucose regulation, since it is also responsible for circulating insulin levels by extracting about 50% of insulin appearing in the portal circulation, with every passage through it. A quantitative estimation of hepatic insulin extraction (HE), both in basal and dynamic physiological conditions (such as after an oral glucose load) is therefore a key aspect for a systematic description of glucose metabolism. Since a direct measurement of HE is very invasive, requiring the insertion of catheters

into the portal and hepatic veins, indirect methods employing mathematical models are used. Such models require measurement of plasma concentrations and knowledge of the kinetics of C-peptide, and insulin secretion and clearance. This is facilitated by the fact that insulin and C-peptide are secreted in a 1:1 ratio by the beta-cells, and that the liver extracts insulin, but not C-peptide.

The first model available in the literature for assessing HE was developed by Toffolo et al. and describes HE during an insulin modified intravenous glucose tolerance test (IM-IVGTT); this model estimates the insulin secretion rate (ISR) and the insulin delivery rate (IDR) from C-peptide and insulin concentrations, respectively. HE is subsequently derived from these two fluxes. More recently, Campioni et al. proposed a model to estimate HE after meal ingestion. In this case HE is described as a piecewise linear function, with a fixed number of breakpoints, which are the model parameters to be estimated. The main limitation of this approach is that, although allowing a reconstruction of the HE profile, it does not provide a mechanistic relationship between the involved variables, and thus the resulting model parameters do not have an easy physiological interpretation. Moreover, model structure makes the parameter identification vulnerable to noise, since the HE profile may vary rapidly to fit fluctuations in peripheral insulin concentrations.

The aim of this work is to overcome the disadvantages of the available HE description by proposing a new physiological model of insulin kinetics and extraction. The best model is selected from seven, including an increasing number of compartments and different mechanistic descriptions of HE, each taking into account the influence of one or more modifiers, such as plasma glucose and insulin concentrations. In fact, during an oral test, one observes that, while glucose and insulin concentrations rise, the HE time course decreases in the meantime. These models are tested against data of a frequently sampled mixed meal (21 plasma samples) measured in 204 healthy subjects. The best model was selected according to standard criteria (ability to describe the data, precision of parameter estimates, model parsimony). Such a model describes insulin kinetics with three compartments, and HE

as a function of plasma glucose concentration. One of the peculiarities of this model is to provide an index of HE sensitivity to glucose (S_G^{HE}), besides total (HE_{tot}) and basal (HE_b) HE indexes, already adopted in the literature. Moreover, the new model performs well even in data sets with less frequent sampling (11 samples).

The new model was then applied to three further databases, involving subjects with different degrees of glucose tolerance, studied with a standard mixed meal or the oral glucose tolerance test (OGTT). The first data set is composed of 62 prediabetic subjects (including healthy, glucose intolerant subjects, and subjects with impaired fasting glucose), who underwent a triple tracer mixed meal and an OGTT. The model was able to describe data during both the tests, and HE indexes are shown to correlate with the degree of dysfunction in glucose metabolism. The second data set consists of 11 healthy and 14 T2DM subjects, matched for age, weight and body mass index (BMI), who underwent a mixed meal test with the triple tracer technique. Also in this case, the new model predicts the data, and the estimated HE indexes (HE_b, HE_{tot}, S_G^{HE}) differ significantly between the two groups. The last database is composed of 14 subjects with T2DM who were treated with vildagliptin or placebo before the meal; moreover, at t = 300 min, 0.02 unit/kg insulin was administered intravenously (over a 5-min period), thus allowing a better estimation of insulin kinetics. In this case the model was used in two different ways: at first, analyzing all the available plasma samples, then, neglecting the insulin infusion and just considering the former part of the test. Interestingly, the model provided a good correlation among the HE parameters in these two different occasions.

In summary, we have developed a model of insulin kinetics which contains a new physiological description of HE. This model allows a good prediction of the available data during meals and OGTT in all the spectrum of glucose tolerance (healthy, intolerant and T2DM), also providing a powerful new index of HE sensitivity to glucose.

Italiano

La regolazione del metabolismo del glucosio, in soggetti sani, si basa su un complesso sistema di controllo, che mira a mantenerne la concentrazione plasmatica in un range limitato ($70 \div 180$ mg/dl). L'insulina, un ormone secreto dalle beta-cellule pancreatiche, ha un ruolo fondamentale nell'omeostasi del glucosio, riducendone la produzione epatica, e stimolandone l'utilizzazione da parte degli organi insulino-dipendenti. L'incapacità da parte delle beta-cellule di secernere adeguatamente l'insulina può creare problemi metabolici, che possono anche provocare uno stato di intolleranza al glucosio, o addirittura il diabete mellito. Esistono due diversi tipi di diabete: il diabete di tipo 1 (T1DM), caratterizzato da una totale impossibilità di secernere insulina da parte delle beta-cellule pancreatiche, e il tipo 2 (T2DM), in cui, a causa dell'insulino-resistenza, i tessuti non riescono a utilizzare adeguatamente il glucosio, e la secrezione insulinica è insufficiente per compensare questo difetto. Data la crescente diffusione del diabete, comprendere tutti i meccanismi coinvolti nel sistema di regolazione del glucosio è molto importante.

Il fegato è un organo fondamentale nella regolazione del glucosio, poichè è anche responsabile dei livelli di insulina plasmatica, estraendone circa il 50% dalla circolazione portale, ad ogni passaggio attraverso di esso. La quantificazione dell'estrazione insulinica epatica (HE), sia in condizioni basali che in condizioni dinamiche (come per esempio dopo un carico orale di glucosio), è quindi fondamentale per descrivere il metabolismo del glucosio. Dato che una misura diretta di HE è molto invasiva, richiedendo l'inserzione di cateteri nella vena porta e epatica, si preferisce utilizzare metodi indiretti, basati sui modelli matematici. Tali modelli richiedono misure delle concentrazioni plasmatiche, e la conoscenza della cinetica del C-peptide, della secrezione e della degradazione dell'insulina. È infatti noto che insulina e C-peptide sono secreti in maniera equimolare dalle beta-cellule pancreatiche, ma soltanto l'insulina viene poi estratta dal fegato.

Il primo modello disponibile in letteratura per descrivere HE è stato sviluppato da Toffolo et al., e descrive HE durante un insulin-modified intraven-

ous glucose tolerance test (IM-IVGTT); questo modello fornisce una stima della secrezione insulinica (ISR) e della velocità di comparsa dell'insulina nel plasma (IDR), rispettivamente dalle concentrazioni di C-peptide e insulina. HE viene quindi calcolata da questi due flussi. Più recentemente, Campioni et al. hanno proposto un modello di stima di HE durante pasto. In questo caso HE è descritta come una funzione lineare a tratti, con un numero prefissato di punti, che sono i parametri stimati dal modello. La limitazione principale di questo approccio è che, benchè il profilo di HE venga ricostruito, non è fornita una relazione meccanicistica tra le variabili coinvolte, e quindi i parametri del modello non hanno un'immediata interpretazione fisiologica. Inoltre, la struttura del modello rende l'identificazione parametrica sensibile al rumore, poichè il profilo di HE può essere soggetto a rapide variazioni a seguito delle fluttuazioni della concentrazione di insulina periferica.

Lo scopo di questo lavoro è quindi di superare gli svantaggi della descrizione di HE attualmente disponibile, proponendo un nuovo modello fisiologico della cinetica e estrazione dell'insulina. Il modello migliore viene selezionato tra sette nuovi modelli, che includono un numero di compartimenti crescente, e diverse descrizioni fisiologiche di HE, ciascuna contenente l'influenza di uno o più controlli, come le concentrazioni plasmatiche di glucosio e insulina. Infatti, durante un test orale è possibile osservare che, mentre le concentrazioni di glucosio e insulina salgono, il profilo temporale di HE decresce. Questi modelli sono stati testati in 204 soggetti sani studiati con un pasto misto e campionato frequentemente (21 campioni). Il modello migliore è quindi stato selezionato in base a criteri standard (abilità di predizione dei dati, precisione delle stime parametriche, parsimonia). Tale modello risulta comprendere una descrizione della cinetica dell'insulina a tre compartimenti, dove HE è funzione della concentrazione di glucosio. Una delle peculiarietà del modello è la possibilità di ottenere un indice di sensibilità di HE al glucosio (S_G^{HE}), oltre agli usuali indici basale (HE_b) e totale (HE_{tot}) di HE, già presenti in letteratura. Inoltre, il nuovo modello fornisce buone performance anche in dati raccolti con un campionamento standard, quindi meno frequente (11 campioni).

Il modello selezionato è stato quindi utilizzato in altri tre diversi database, costituiti da soggetti con vari gradi di tolleranza al glucosio, studiati durante un pasto misto standard, o un test orale di tolleranza al glucosio (OGTT). Il primo data set impiegato è composto da 62 soggetti prediabetici (ovvero sani, intolleranti al glucosio, e soggetti con ridotta glicemia a digiuno), sottoposti sia a un pasto misto con triplo tracciante, sia a un OGTT. Il modello si è dimostrato in grado di descrivere i dati adeguatamente durante entrambi i test, e gli indici di HE mostrano una correlazione con il grado di disfunzione nel metabolismo del glucosio. Il secondo data set consiste di 11 soggetti sani e 14 T2DM, di simile età, peso e indice di massa corporea (BMI), sottoposti a pasto misto con triplo tracciante. Anche in questo caso il nuovo modello è in grado di predire i dati, e gli indici di HE (HE_b, HE_{tot}, S_G^{HE}) risultano significativamente diversi nei due gruppi. L'ultimo database è costituito da 14 soggetti T2DM, trattati sia con vildagliptin che con placebo prima del pasto; inoltre in t = 300 min, sono state somministrate 0.02 unità/kg di insulina per via endovenosa (in un periodo di 5 minuti), permettendo quindi una migliore stima della cinetica dell'insulina. In questo caso il modello è stato usato in due modi differenti: prima analizzando tutti i campioni plasmatici a disposizione, quindi, successivamente, trascurando l'infusione di insulina, e considerando solo la parte iniziale del test. Un risultato interessante riguarda il fatto che il modello fornisce una buona correlazione tra i parametri di HE, calcolati nelle due diverse identificazioni.

Quindi, riassumendo, è stato sviluppato un modello della cinetica dell'insulina, contenente una nuova descrizione fisiologica di HE. Questo modello permette una buona predizione dei dati disponibili durante pasto e OGTT, in tutto lo spettro di tolleranza al glucosio (soggetti sani, intolleranti e T2DM), fornendo inoltre un nuovo indice di sensibilità di HE al glucosio.

Glossary

ADA	American Diabetes Association
BMI	Body Mass Index
BSA	Body Surface Area
CRU	Clinical Research Unit
CV	Coefficient of Variation
DM	Diabetes Mellitus
E	Elderly
EM	Elderly Men
EW	Elderly Women
FFA	Free Fatty Acids
FPG	Fasting Plasma Glucose
GIP	Glucose-dependent Insulinotropic Peptide
GLP-1	Glucagon-like Peptide 1
FS	Frequent Sampling
HE	Hepatic Insulin Extraction
IDE	Insulin Degrading Enzyme
IDR	Insulin Delivery Rate
IFG	Impaired Fasting Glucose
IGT	Impaired Glucose Tolerance
IM-IVGTT	Insulin Modified Intravenous Glucose Tolerance Test
ISR	Insulin Secretion Rate
IVGTT	Intravenous Glucose Tolerance Test
MTT	Meal Tolerance Test
NFG	Normal Fasting Glucose

NGT	Normal Glucose Tolerance
nWRSS	normalized Weighted Residuals Square Sum
OGTT	Oral Glucose Tolerance Test
SE	Standard Error
SS	Standard Sampling
T2DM	Type 2 Diabetes
Y	Young
YM	Young Men
YW	Young Women
WRSS	Weighted Residuals Square Sum

1 Introduction

1.1 Background

The regulation of glucose metabolism is based on a complex control system that, in healthy conditions, aims to maintain plasma glucose concentration within a narrow range (from 70 to 180 mg/dl), over the whole day. Therefore, the correct operation of this control is fundamental, in order to avoid plasma glucose levels falling below 70 mg/dl, or rising over 180 mg/dl, causing hypoglycemia or hyperglycemia, respectively [18]. Both these abnormal states have adverse consequences. Hypoglycemia may cause impaired brain function, due to an inadequate glucose provision, which can result in dysphoria, but also seizures, unconsciousness, and death. Hyperglycemia is problematic as well, since it can be associated with chronic states, leading to cardiac, neuronal, renal and retinal diseases [18, 23]. Therefore, a complete understanding of all the mechanisms involved in the glucose metabolism regulation is essential.

Plasma glucose concentration results from the balance of the rate of glucose entering the circulation (glucose rate of appearance, R_a), and the rate of its removal from the circulation (glucose rate of disappearance, R_d). Blood glucose is mainly provided by three different sources: intestinal absorption during the fed state, glycogenolysis, and gluconeogenesis. Glycogenolysis and gluconeogenesis are hepatic processes, stimulating, respectively, the break-

down of glycogen as a storage form of glucose, and the formation of glucose from lactate and aminoacids during the fasting state; both processes are partly controlled by glucagon, a hormone produced by the pancreatic alpha-cells.
In the first $8 \div 12$ hours of fasting, glycogenolysis is the primary mechanism responsible for glucose availability. This process is stimulated by glucagon, thus promoting glucose appearance in the circulation. Over longer periods of fasting, glucose coming from gluconeogenesis is released from the liver [2].

Many hormones are involved in the glucose regulatory system: insulin, glucagon, amylin, Glucagon-like Peptide 1 (GLP-1), glucose-dependent insulinotropic peptide (GIP), epinephrine, cortisol, and growth hormone. Among them, insulin and amylin are secreted by the pancreatinc beta-cells, glucagon by the pancreatic alpha-cells, GLP-1 and GIP by the intestinal L-cells [2].
Insulin is considered the main hormone responsible for glucose homeostasis, since it provides a hypoglycemic effect, by decreasing liver and kidney glucose production, while promoting its utilization by the insulin-dependent organs (skeletal muscles and adipose tissues), and suppressing the post-prandial glucagon secretion. Normally, it is secreted in response to increased blood glucose and aminoacids following ingestion of a meal, while it is not secreted when glucose levels are ≤ 60 mg/dl [2].
Glucagon effect is opposite that of insulin, since it is responsible for raising plasma glucose concentrations, when hypoglycemia occurs. It plays a major role in sustaining plasma glucose during fasting conditions by stimulating hepatic glucose production and gluconeogenesis. On the other hand, immediately after a meal, an endogenous source of glucose is not needed, and thus glucagon secretion is suppressed.
Acting together, glucagon and insulin make up a feedback system that regulates blood glucose levels [2].

The inability of this control system to adequately work creates metabolic disorders which can result in different degrees of glucose intolerance or diabetes mellitus. Diabetes is a social pathology, characterized by chronic

hyperglycemia, in which insulin secretion and action are not sufficient to maintain blood glucose levels in the normal range. As a result, postprandial glucose concentrations rise due to lack of insulin-stimulated glucose disappearance, poorly regulated hepatic glucose production, and increased or abnormal gastric emptying following a meal. There are two different kinds of diabetes: type 1 diabetes (T1DM), and type 2 diabetes (T2DM).

T1DM, afflicting 5÷10% of all the diabetic population, also known as "insulin-dependent", is characterized by the inability of pancreatic beta-cells to secrete insulin, as a consequence of their immune-mediated destruction. This kind of pathology mostly arises in children and adolescents, and is thus called juvanile diabetes. The absolute lack of insulin causes hyperglycemia because of an impaired hepatic glucose production regulation, and an interruption of glucose utilization; therefore exogenous insulin administration is necessary, in order to compensate for the lack of a correct glucose control.

T2DM, afflicting 90÷95% of all the diabetic population, is also known as "insulin-independent"; tissues are unable to appropriately utilize glucose because of insulin resistance, and insulin secretion cannot compensate for this. Being insulin secretion impaired, even if not completely absent, it is always possible to find circulating insulin; nevertheless, T2DM causes hyperglycemia, too. This kind of pathology especially arises in adult and elderly people, and it is often associated with obesity. Typical therapies for T2DM concern an improvement of lifestyle, consisting of a regular diet and physical exercise; sometimes also drugs are necessary (metformin, sulfonylureas, meglitinides, thiazolidinediones and many others), as well as an insulin treatment.

Diabetes mellitus is characterized by highly invalidating complications, that, in the long term, can cause serious pathologies, as such as cardiovascular diseases, retinopathy, kidney's disorders, impotence, neuropathy and nephropathy. The International Diabetes Federation (IDF) estimates that 8.3% of adults (382 million people) have diabetes, and the number of affected people is set to rise beyond 592 million in less than 25 years [33], that is why diabetes is considered a social pathology.

T2DM is often preceded by prediabetes, characterized by an impaired gluc-

ose control which can make plasma glucose level rise, even if the consequent hyperglycemia is not enough to be considered diabetes. The prediabetes diagnosis is usually performed by two different tests: the fasting plasma glucose test (FPG), and the oral glucose tolerance test (OGTT). The FPG, according to the ADA criteria [18], allows to distinguish normal fasting glucose (NFG, blood glucose level $\leq$ 5.2 mmol/l) and impaired fasting glucose subjects (IFG, blood glucose level between 5.2 mmol/l and 7 mmol/l). IFG is thus considered an early form of diabetes, and its severity can be classified by using the OGTT, understanding whether people are affected by normal glucose tolerance (NGT), impaired glucose tolerance (IGT), or diabetes (DM). Subjects with IFG are at 20$\div$30% risk of progressing to T2DM in the following 5$\div$10 years; this risk is even higher if they are also affected by IGT.
Given the increasing prevalence of all the spectrum of glucose intolerance pathologies, a complete understanding of all the mechanisms involved in the glucose regulation system is fundamental.

The liver plays an essential role in glucose metabolism since, beside producing glucose, it is also the main site of insulin extraction. In fact, the amount of insulin reaching the systemic circulation is dependent not only on beta-cell secretion, but also on hepatic insulin extraction, since approximately 50% of the endogenous secreted insulin is removed from the portal circulation by the liver during its first-pass transit [12], even if this percentage varies under different conditions.
Insulin degradation has been overlooked for a long time, but it is really important, because it contributes to the cellular control on insulin, and it is thus related to insulin action. It has been demonstrated that insulin has a short half-life (4$\div$6 min), so it needs to be promptly removed, according to the blood glucose variations [21].
Hepatic insulin uptake is not a static process, because it is influenced by physiological and pathological factors, involving several different systems and controls [21]. It is a receptor-mediated mechanism, in which high insulin concentrations stimulate a decrease of fractional uptake, even if the total uptake is increased [22, 35]. Moreover, high portal insulin levels cause an impaired clearance, due to receptor down-regulation.

However, it is important to remark that insulin removal from plasma circulation does not implicate its sudden destruction, since a significant portion of it can then be released from the cells, and thus reenter the blood circulation. For example, the muscles can capture, and then release insulin back into the circulation [22].
A further important aspect concerning the alterations of insulin clearance, is nutrient intake. In general, it has been demonstrated that the oral glucose ingestion, differently from the portal infusion, can increase the hepatic insulin uptake process, probably because of the presence of gut signals. However glucose, by increasing insulin secretion, may also decrease the hepatic insulin extraction [21]. Also free fatty acids (FFA) may interfere with hepatic insulin degradation, to such an extent that they may be involved in the pathogenesis of T2DM, by inhibiting insulin binding, degradation and action in the liver [49].
Hepatic insulin clearance has been demonstrated to decrease in obese and diabetes patients. Furthermore, liver disease may also cause a decrease in hepatic insulin degradation, which could consequently be associated with reduced insulin sensitivity, thus supporting the strong connection between it and the whole insulin action [49].
For all these reasons, hepatic insulin extraction, by removing and inactivating insulin, has an important role in the glucose regulation system.

1.2 Aim

The general aim of this thesis is to develop a new oral model for the estimation of hepatic insulin extraction, which is able to describe insulin secretion and kinetics in all the spectrum of glucose tolerance (healthy, prediabetic, and T2DM subjects).
In particular, the specific tasks of this work are:

- To choose an optimal model of hepatic insulin extraction in healthy subjects that underwent a meal.

- To use the model in prediabetic subjects, as well as in T2DM subjects, also testing its performance during an OGTT.
- To compare the results obtained by considering different pathology levels.

1.3 Outline

This thesis is organized as follows:

- *Chapter 2* provides a basic overview on the physiological processes involved into the hepatic insulin uptake and degradation, at a cellular level.
- *Chapter 3* summarizes the most recent mathematical models proposed in the literature, used to quantify hepatic insulin extraction.
- *Chapter 4* describes all the databases involved in this thesis, as well as all the experimental protocols.
- *Chapter 5* presents the new insulin kinetics and hepatic insulin extraction models, proposed in this work.
- *Chapter 6* reports all the model selection process, in healthy subjects, during a meal test.
- *Chapter 7* contains the results obtained by using the selected models in prediabic and T2DM subjects, during meal and OGTT.

The results of this thesis, as well as all the possible future developments and open questions, are discussed in the *Conclusions*.

2 Hepatic insulin uptake and degradation

2.1 Introduction

As mentioned in chapter 1, the liver, and thus the hepatocytes, account for the majority of the insulin uptake and degradation, even if this process is also peculiar to all insulin-sensitive tissues; thus insulin is endocytosed and degraded in most cell types (for example, adipocytes and fibroblasts). In this chapter, a brief overview of the cellular mechanisms of insulin uptake and degradation is provided.

2.2 Insulin uptake and degradation

The insulin degradation process is very complex and has multiple components, thus the topic is still very controversial. The process is sequential, involving an initial reductive cleavage of the insulin molecule, with subsequent proteolysis of separate chains [21].
Cellular insulin internalization can be operated by pinocytosis, especially when its concentration is high [21], but the main mechanism of cellular uptake is a receptor-mediated system.
The first step is the insulin binding by its receptors (see Fig. 2.1), which creates an insulin reserve that can either return to the circulation, or be

transported to an intracellular site [29]. Multiple pathways are possible: insulin can either be degraded in endocytotic vesicles [3, 48], or, alternatively, it can remain intact, and be released from the cells by diacytosis or retroendocytosis to other subcellular sites.
The main locations of internalized insulin are the cytosol, nucleus, and Golgi [21], in which insulin can be directly degraded, or delivered to lysosomes for the ultimate degradation step [45]. Also partially degraded insulin can return to the circulation [38], retaining receptor binding and biological activity [58].

The receptor-bound insulin is usually internalized into the cellular endosomes [28], by an energy-requiring adsorbitive endocytosis, and then the degradation process starts. After their formation, the endosomes quickly acidify, and insulin is thus dissociated from the receptor within the vescicle. Insulin degradation begins just before the acidification mechanism [28], thanks to the specific insulin degrading enzyme (IDE). The receptor-bound insulin is a substrate for IDE [20], that is present in endosomes, but also in cytosol, plasma membranes, and peroxisomes [21]; it is responsible for starting the cellular insulin process, and degrading of a significant portion of it on the cell membrane.
There is evidence that suggests that IDE overexpression regulates cellular insulin degradation by increasing the process [36].
Insulin-IDE interactions are very important since many studies support the hypothesis that they could modulate fat and protein metabolism [21].
The quantification of endosomes degradation is variable, depending on insulin concentration, duration of exposure, and many other factors [43]. Typically, 50% of insulin amount is degraded, and the remaining portion is delivered to other subcellular compartments, as such as cytosol, nucleus and lysosomes [30], using pathways which involve IDE action [1].
While the first degradation occurring immediately after cells exposure to insulin takes place in endosomes, the fraction of insulin that remains intact, or just partially degraded, is then carried to the lysosomes, where it is finally metabolized [21].
After the degradation products are released into the medium by exocytosis,

the receptor is recycled in a vescicle to the plasma membrane, so that, normally, no accelerated net consumption of the receptor takes place [46].
It is important to remark that some studies have noticed a "downregulation" of the degradation process, operated by insulin: the hyperinsulinemic state induces a loss of receptors, or makes them unavailable for binding and endocytosis, i.e. insulin induces an acceleration of the rate of receptors degradation in some tissues, without altering their rate of synthesis, leading to a reduced number of receptors.

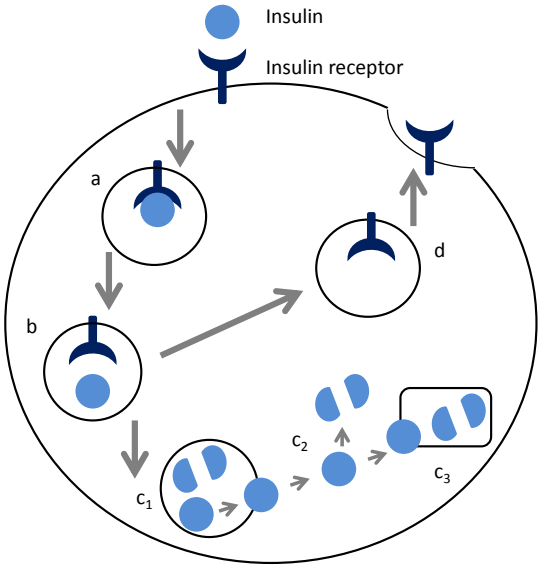

Figure 2.1: Pathways for the internalization and processing of insulin. After insulin binds to its plasma membrane receptor, it is internalized in a endocytic vescile (a). This vesicle then undergoes acidification, which causes the insulin to dissociate from its receptor (b). Insulin is then degraded in endosomes (c_1), or traslocated to cytosol and degraded there (c_2), or delivered to other subcellular compartments, as such as peroxisomes (c_3). The receptor is recycled in a vescicle to the plasma membrane (d). Adapted from [37].

3 State of the art models of hepatic insulin extraction

3.1 Introduction

In this Chapter two models, previously proposed for assessing hepatic insulin extraction (HE), are described: an IM-IVGTT and an oral model. Afterwords, their limitations are highlighted.

As previously mentioned, the liver plays a fundamental role in glucose metabolism since, besides producing glucose, it is responsible of regulating insulin levels by extracting a significant fraction of the secreted insulin. Previous studies have demonstrated that the liver removes about 50% of insulin appearing in the portal circulation, at every passage through it. Therefore, the assessment of hepatic insulin extraction, in the basal state as well as in dynamic situations, is a crucial point for completely understanding the glucose metabolism [15].

The HE process appears to be dynamic and is affected by, amongst other parameters, the amplitude of portal insulin pulses [39], circulating free fatty acids [57], and hyperglycemia per se [21]. Unfortunately, a direct measurement of HE is very invasive, requiring the insertion of catheters into the portal and hepatic veins, respectively. For these reasons, the estimation of HE using mathematical models, despite being an indirect method (since usu-

ally models employ plasma concentration measurements), is more applicable to well-powered studies in humans [26]. Such models are based on the evidence that C-peptide and insulin are secreted into the portal vein in equimolar concentrations by the beta-cells and the fact that the liver extracts insulin, but not C-peptide. Thus, from plasma C-peptide and insulin concentrations it is possible to make inferences on the process of HE.

Several models estimating HE after an oral or intravenous glucose perturbation are available in the literature [14, 24, 53, 56], but they suffer from two main limitations. First of all, the simultaneous estimation of secretion and kinetics negatively affects the assessment of the secretion, because of possible unexpected parameter compensations [52]. Secondly, the fact that HE is sometimes considered a constant variable is not realistic, since there is evidence of its variability with time [53].

3.2 Models

3.2.1 The IM-IVGTT model

Toffolo et al. [50] proposed a model for the assessment of HE during an IM-IVGTT.
This method employs the minimal model of C-peptide secretion and kinetics [24], coupled with a model of insulin kinetics [50]. This last is well identifiable during an IM-IVGTT thanks to the square-wave insulin infusion administrated 20 min after the glucose bolus [51].

The C-peptide minimal model. C-peptide kinetics is described by a two compartment model [24] (as shown in Fig. 3.1):

$$\dot{CP}_1(t) = -(k_{01} + k_{21}) \cdot CP_1(t) + k_{12} \cdot CP_2(t) + isr(t) \qquad CP_1(0) = C_{1b} \tag{3.1}$$

$$\dot{CP}_2(t) = -k_{12} \cdot CP_2(t) + k_{21} \cdot CP_1(t) \qquad CP_2(0) = \frac{C_{1b} \cdot k_{21}}{k_{12}} \tag{3.2}$$

$$CP(t) = CP_1(t) \tag{3.3}$$

where CP_1 and CP_2 (pmol/l) are C-peptide concentrations in the accessible and in the peripheral compartment, respectively, CP (pmol/l) is the measured C-peptide concentration, C_{1b} (pmol/l) the end test C-peptide concentration, k_{01}, k_{21}, k_{12} (min^{-1}) rate transfer parameters, and isr (pmol/l/min) is the secretion rate, normalized by the volume of distribution of compartment 1, V_c (l).

isr is assumed to be proportional to the amount of insulin contained in the

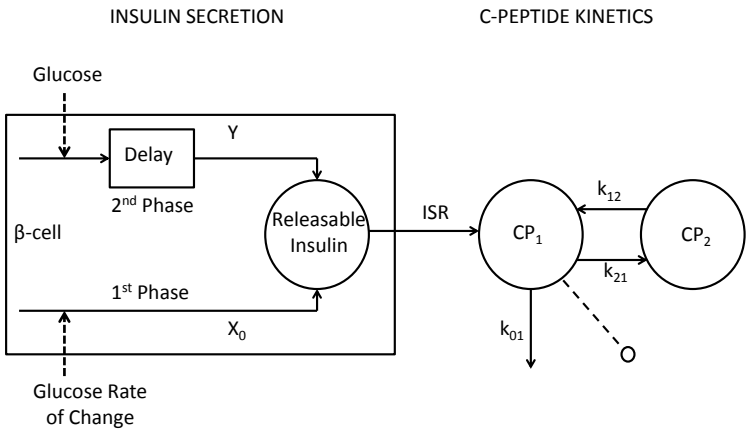

Figure 3.1: Minimal model of C-peptide secretion and kinetics during an IM-IVGTT. CP_1 and CP_2 (pmol/l), plasma C-peptide concentrations in the accessible and peripheral compartments; k_{01}, k_{12}, k_{21} (min^{-1}), rate transfer parameters; ISR (pmol/min), insulin secretion rate; Y (pmol/l/min), new insulin provision; X_0 (pmol/l), first phase secreted insulin.

beta-cells, X (pmol/l), which is related to the provision of new insulin in the

beta-cells, Y (pmol/l/min), with a first order differential equation:

$$isr(t) = m \cdot X(t) + k_{01} \cdot C_{1b} \tag{3.4}$$

$$\dot{X}(t) = -m \cdot X(t) + Y(t) \quad X(0) = X_0 \tag{3.5}$$

X_0 accounts for the first-phase secretion, while the second-phase derives from Y and is controlled by glucose:

$$\dot{Y}(t) = -\alpha \cdot \{Y(t) - \beta \cdot [G(t) - h]\} \quad Y(0) = 0 \tag{3.6}$$

Evidently from Eq. (3.6), when the glucose level is high, Y and isr tend with a rate constant $1/\alpha$ (min) towards a steady state which is linearly related to glucose concentration G above the threshold level h, via the parameter β.
The total insulin secretion rate, ISR (pmol/min), is reconstructed as follows:

$$ISR(t) = isr(t) \cdot V_c = [k_{01} \cdot C_{1b} + m \cdot X(t)] \cdot V_c \tag{3.7}$$

This model allows the calculation of indexes representing basal secretion, as well as the first and second-phase beta-cell responsivity to glucose. The basal secretion index Φ_b (10^{-9} min^{-1}) is defined as:

$$\Phi_b = isr_b/G_b = k_{01} \cdot C_{1b}/G_b \tag{3.8}$$

where G_b is the end-test glucose concentration.
Φ_1 (10^{-9}) is the first-phase glucose responsivity index, calculated as:

$$\Phi_1 = X_0/\Delta G \tag{3.9}$$

where ΔG (mmol/l) is maximum glucose increment above basal.
The second-phase glucose responsivity index, Φ_2 (10^{-9} min^{-1}), which describes the stimulation of insulin provision, operated by glucose, is calculated as:

$$\Phi_2 = \beta \tag{3.10}$$

The insulin minimal model. Insulin kinetics is well described by a single-compartment model [50] (see Fig. 3.2):

$$\dot{I}(t) = -n \cdot I(t) + idr(t) + U(t)/V_I \quad I(0) = I_b \tag{3.11}$$

where I_b (pmol/l) and I (pmol/l) are, respectively, the end-test and the measured insulin concentration, n (min^{-1}) is the rate constant of insulin disappearance, idr (pmol/l/min) is the insulin delivery rate, normalized by insulin volume of distribution V_I (l), and U (pmol/min) is the exogenous insulin infusion, usually administrated in the $20 \div 25$ min interval. According to [50], idr is here described similarly to isr:

$$idr(t) = m^{IDR} \cdot X^{IDR}(t) + n \cdot I_b \tag{3.12}$$

$$\dot{X}^{IDR}(t) = -m^{IDR} \cdot X^{IDR}(t) + Y^{IDR}(t) \qquad X^{IDR}(0) = X_0^{IDR} \tag{3.13}$$

$$\dot{Y}^{IDR}(t) = -\alpha^{IDR} \cdot \{Y^{IDR}(t) - \beta^{IDR} \cdot [G(t) - h]\} \quad Y^{IDR}(0) = 0 \tag{3.14}$$

where the apex "IDR" indicates that parameters refer to insulin delivery rate, i.e. they combine both insulin secretion rate and hepatic extraction.
IDR (pmol/min) can be obtained as:

$$IDR(t) = idr(t) \cdot V_I = [n \cdot I_b + m^{IDR} \cdot X^{IDR}] \cdot V_I \tag{3.15}$$

Insulin delivery rate indexes of basal, first- and second-phase responsivity to glucose were calculated, similarly to Eq. (3.8), (3.9), (3.10):

$$\Phi_b^{IDR} = idr_b/G_b = n \cdot I_b/G_b \tag{3.16}$$

$$\Phi_1^{IDR} = X_0^{IDR}/\Delta G \tag{3.17}$$

$$\Phi_2^{IDR} = \beta^{IDR} \tag{3.18}$$

where G_b is the end-test glucose concentration.
Using ISR and IDR time courses it is possible to reconstruct the HE profile, as well as indexes of basal (HE_b) and a total (HE_{tot}) hepatic insulin

extraction:

$$HE(t) = \frac{ISR(t) - IDR(t)}{ISR(t)} = 1 - \frac{IDR(t)}{ISR(t)} \tag{3.19}$$

$$HE_b = \frac{isr_b \cdot V_c - idr_b \cdot V_I}{isr_b \cdot V_c} = 1 - \frac{\Phi_b^{IDR} \cdot V_I}{\Phi_b \cdot V_c} \tag{3.20}$$

$$\begin{aligned} HE_{tot} &= \frac{\int_0^T ISR(t)dt - \int_0^T IDR(t)dt}{\int_0^T ISR(t)dt} \\ &= 1 - \frac{(\Phi_b^{IDR} + \Phi_1^{IDR} \cdot A_1 + \Phi_2^{IDR} \cdot A_2) \cdot V_I}{(\Phi_b + \Phi_1 \cdot A_1 + \Phi_2 \cdot A_2) \cdot V_c} \end{aligned} \tag{3.21}$$

$$A_1 = \frac{\Delta G}{T \cdot G_b} \tag{3.22}$$

$$A_2 = \frac{\int_0^T [G(t) - h]dt}{T \cdot G_b} \tag{3.23}$$

where T is the duration of the experiment.

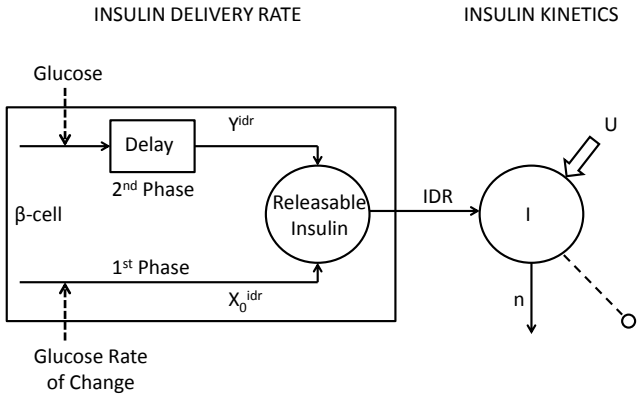

Figure 3.2: Minimal model of insulin secretion and kinetics during an IM-IVGTT. I (pmol/l), plasma insulin concentration; n (min^{-1}), rate constant of insulin disappearance; U (pmol/min), exogenous insulin infusion; IDR (pmol/min), posthepatic insulin delivery rate; Y^{idr} (pmol/l/min), comparable to new insulin provision; X_0^{idr} (pmol/l), first-phase secreted insulin.

It is of note that in this model the C-peptide kinetic parameters (V_c, k_{12}, k_{01}, and k_{21}) are fixed in each subject, according to the anthropometric

characteristics (BSA and BMI), as proposed in [55], in order to avoid possible compensations among secretion and kinetic parameters. For insulin, the estimation of both kinetics and IDR was made possible thanks to the peculiarity of the IM-IVGTT protocol, in which an insulin concentration decay can be measured after the short insulin infusion.

3.2.2 The oral model

In order to extend the approach used by Toffolo et al. in [50] to assess HE during a more physiological oral glucose test, Campioni et al. [11] proposed a single-compartment insulin minimal model to assess IDR, here named *Model of Data*, due to the piecewise linear description of HE [see Eq. (3.34) later]. For C-peptide kinetics and secretion, previous models available in literature were used [10, 24].

The C-peptide minimal model. C-peptide kinetics is described by the same two-compartment model shown in Eq. (3.1)-(3.2) [24].
The pancreatic secretion ISR (pmol/min) is described as the sum of three different components [10] (see Fig. 3.3): basal ISR_b, static ISR_s, proportional to glucose concentration, and dynamic ISR_d, proportional to glucose rate of increase:

$$ISR(t) = ISR_b + ISR_s(t) + ISR_d(t) \tag{3.24}$$

ISR_b can be obtained from steady state constraint of (3.24):

$$ISR_b = CP_b \cdot k_{01} \cdot V_c \tag{3.25}$$

ISR_s represents the provision of releasable insulin controlled by glucose concentration G (mmol/l) in a linear dynamic way: if plasma glucose shows a step increase above a threshold level h (mmol/l), the provision tends with a rate constant α (min^{-1}), and thus with a delay $\text{T} = 1/\alpha$ (min), toward a steady-state value that is linearly dependent to the glucose step through a

parameter β (10^{-9} min^{-1}):

$$I\dot{S}R_s(t) = -\alpha \cdot [ISR_s(t) - V_c \cdot \beta.(G(t) - h)] \quad ISR_s(0) = 0 \tag{3.26}$$

ISR_d is the secretion of insulin from the promptly releasable pool, and it is proportional to the rate of increase of glucose $\dot{G}$ (mmol/l/min) through the parameter K_d (10^{-9}):

$$ISR_d = \begin{cases} V_c \cdot K_d \cdot \dot{G}(t) & if\, \dot{G}(t) \geq 0 \\ 0 & if\, \dot{G}(t) < 0 \end{cases} \tag{3.27}$$

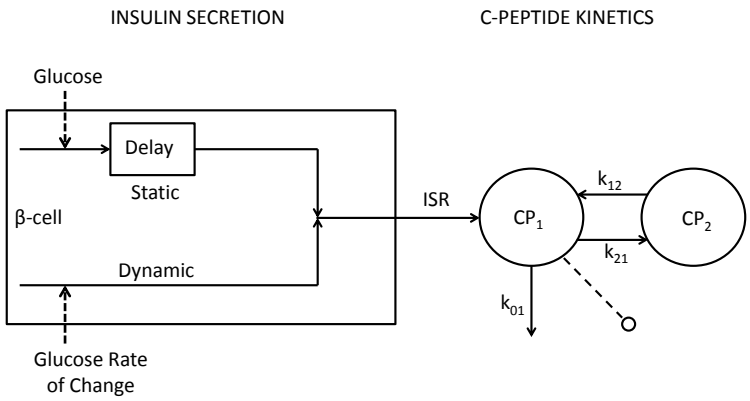

Figure 3.3: Minimal model of C-peptide secretion and kinetics during an oral test. CP_1 and CP_2 (pmol/l), plasma C-peptide concentrations in the accessible and peripheral compartments; k_{01}, k_{12}, k_{21} (min^{-1}), rate transfer parameters; ISR (pmol/min), insulin secretion rate.

The model allows the estimation of the basal, i.e. Φ_b (10^{-9} min^{-1}), static, i.e. Φ_s (10^{-9} min^{-1}), and dynamic, i.e. Φ_d (10^{-9}), indexes of sensitivity to glucose; moreover, a total index Φ_{tot} (10^{-9} min^{-1}) accounting for both the static and dynamic component can be obtained.
Φ_b, similarly to Eq. (3.8), is defined as:

$$\Phi_b = isr_b/G_b = k_{01} \cdot CP_b/G_b \tag{3.28}$$

where G_b (mmol/l) and CP_b (pmol/l) are, respectively, basal glucose and C-peptide concentrations.
Φ_s measures effect of glucose on beta-cell secretion and is thus defined as the ratio between ISR and glucose concentration above basal at steady state; it can be easily calculated as:

$$\Phi_s = \beta \tag{3.29}$$

Φ_d measures the effect of glucose rate of increase on the secretion of stored insulin; it is defined as the amount of insulin (per unit of C-peptide volume of distribution) released in response to the maximum glucose concentration achieved during the experiment, normalized by the glucose increase; it is obtained as:

$$\Phi_d = K_d \tag{3.30}$$

Φ_{tot} combines Φ_s and Φ_d; it is defined as the average increase above basal of pancreatic secretion over the average glucose stimulus above the threshold level h, and can thus be calculated as:

$$\Phi_{tot} = \Phi_s + \frac{\Phi_d \cdot \Delta G}{\int_0^\infty [G(t) - h]dt} \tag{3.31}$$

where ΔG (mmol/l) is the maximum glucose increment above basal.

The insulin minimal model. Similarly to [50], a linear single-compartment model which describes insulin kinetics [11] is adopted (see Fig. 3.4):

$$\dot{I}(t) = -n \cdot I(t) + idr(t) \quad I(0) = I_b \tag{3.32}$$

where I_b (pmol/l) and I (pmol/l) are, respectively, basal and measured insulin concentration, n (min^{-1}) is the rate constant of insulin clearance, idr (pmol/l/min) is the insulin delivery rate, normalized by insulin volume of distribution V_I (l).

IDR (pmol/min) is the post-hepatic insulin delivery rate, i.e. the fraction

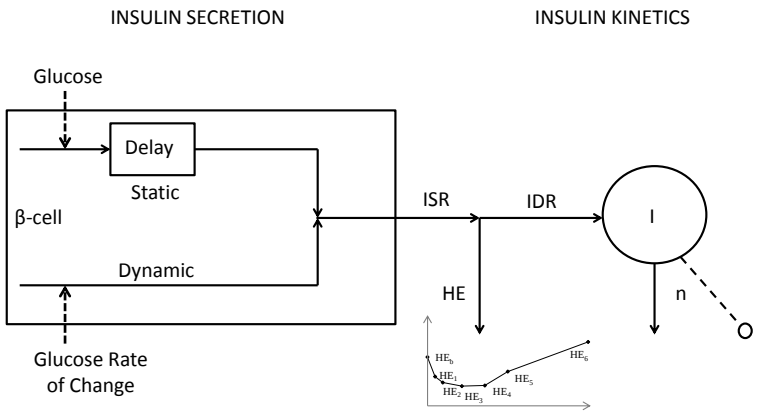

Figure 3.4: Minimal model of insulin secretion and kinetics during an oral test. I (pmol/l), plasma insulin concentration; n (min^{-1}), rate constant of insulin disappearance; ISR (pmol/min), insulin secretion rate; IDR (pmol/min), post-hepatic insulin delivery rate; HE (dimensionless), hepatic insulin extraction.

$(1 - HE)$ of secreted insulin (ISR) which is not extracted by the liver:

$$IDR(t) = ISR(t) \cdot [1 - HE(t)] \tag{3.33}$$

Campioni et al. [11], proposed a parametric description of HE, so that reconstruction of the HE profile is treated as a parameter estimation problem. The most general expression is a piecewise linear function with a given number of breakpoints:

$$HE(t) = \begin{cases} HE_{i-1} + \frac{HE_i - HE_{i-1}}{(t_i - t_{i-1})} \cdot (t - t_i) & t_{i-1} < t < t_i \\ HE_0 = HE_b \end{cases} \tag{3.34}$$

where HE_b is basal hepatic insulin extraction, and HE_i are the parameters to be estimated, representing the values of HE(t) at given time points $i = 1, 2, ..., 6$. $HE(t)$ is supposed to vary more rapidly in the first part of the test, thus the intervals $[t_{i-1}, t_i]$ are shorter at the beginning and longer toward the end (t_i = 0, 20, 40, 90, 150, 210 and 420 min in [11]).
A total index of HE, HE_{tot}, is derived using the first part of Eq. (3.21):

$$HE_{tot} = \frac{\int_0^T ISR(t)dt - \int_0^T IDR(t)dt}{\int_0^T ISR(t)dt} \tag{3.35}$$

while the basal index HE_b, appearing in Eq. (3.34), is obtained from basal ISR and IDR, i.e. from basal insulin and C-peptide concentrations, similarly to Eq. (3.20) as:

$$HE_b = \frac{ISR_b - IDR_b}{ISR_b} = 1 - \frac{I_b \cdot n \cdot V_I}{CP_b \cdot V_c \cdot k_{01}} \tag{3.36}$$

As mentioned in par. 3.2.1, the C-peptide kinetic parameters are fixed according to [55], while for insulin kinetic parameters, linear regression models linking n, V_I and insulin clearance $CL_I = n \cdot V_I$ (l/min) to anthropometric characteristics (BSA and age) were developed [11] (see later, par. 5.5.2). In so doing, it was made possible to estimate insulin kinetic parameters even in databases for which IM-IVGTT data are not available [11].

3.3 Limitations

The model proposed by Toffolo et al. for estimating HE during an IM-IVGTT [50], surely overcomes the problem of undesired parameter estimation compensation due to the simultaneous description of both secretion and kinetics from the same experiment. In fact, as mentioned above, the C-peptide kinetics parameters are fixed to standard values [24], while insulin kinetics and IDR parameters are estimated thanks to the typical IM-IVGTT insulin infusion. However, this model proposes a similar functional description for ISR and IDR, which are both made up of two components: the first phase proportional to the rapid rise in glucose concentrations, and the second phase proportional to the delayed rise in plasma glucose concentration.

The extension of the model proposed by Toffolo et al. to an oral glucose test is not straightforward since the same IDR description cannot be used, and a priori knowledge of insulin kinetics is necessary to assess this flux. For these reasons, Campioni et al. [11] had to initially develop a new model of

IDR, together with a new method for determining standard parameters of insulin clearance, and then, consequently, a new description of HE as a piecewise linear function with a fixed number of breakpoints. At variance with [53], where HE was assumed to be constant during an oral test, Campioni et al. considered it as a time varying profile, according to evidence obtained by measurements using hepatic vein catheterization, which also suggested that HE is strongly related to blood flow [53].
However, the main limitation of this method arises from how HE is described: a piecewise linear function with a given number of breakpoints allows reconstruction of a profile, but does not investigate the mechanistic relationship between the involved variables, and does not provide physiologically meaningful parameters. Moreover, this expression makes the model vulnerable to noise, since the HE profile may rapidly vary to fit fluctuations in peripheral insulin concentrations.

4 Database and Protocols

4.1 Introduction

In this Chapter the databases and protocols, used at first to assess and then to apply the new HE oral model, are described. For the development and selection of the model, a database made up of 204 healthy subjects who underwent a standard mixed meal is used (*database 1*). Then, the abilities of this model are tested across the spectrum of glucose tolerance, employing data of prediabetic subjects (both impaired fasting glucose and impaired glucose tolerant, composing *database 2*) collected during OGTT and mixed meal, and type 2 diabetic subjects (*database 3* and *4*).

4.2 Database 1: healthy subjects

Subjects. The study cohort [6] is made up of 204 healthy subjects [86 elderly men (EM), 59 elderly women (EW), 31 young men (YM), and 28 young women (YW); age 55.5±1.5 yr (means±SE), BMI 26.6±0.2 kg/m^2, BSA 1.90±0.01 m^2], who were in good health and not involved in regular vigorous physical activity.
All subjects consumed a weight maintenance diet (55% carbohydrate, 15%

protein, and 30% fat) for 3 days preceding the study; subsequently, they were admitted to the Mayo Clinic CRU at 1600 on the afternoon before study and had a standard 10-kcal/kg meal (55% carbohydrate, 15% protein, and 30% fat), which was consumed between 1700 and 1730. No additional food was eaten until the next morning.

Mixed meal protocol. At 0600 on the morning of the study, an 18-gauge cannula was put in a retrograde fashion into a dorsal hand vein. The hand was then placed in a heated plexiglas box ($\sim$ 55°C) to obtain arterialized venous blood samples. A further 18-gauge cannula was inserted in the opposite forearm for tracers infusion (not used in this work). At 0900 (0 time), a mixed meal (10 kcal/kg, 45% carbohydrate, 15% protein, and 40% fat) made up of scrambled eggs, Canadian bacon, [1-^{13}C]glucose Jell-O (containing 1.2 g/kg body wt dextrose) was consumed within 15 min, according to [5]. Blood was frequently sampled ($FS\text{-}MTT$) [5] from the arterialized venous site at t = -120, -30, -20, -10, 0, 5, 10, 15, 20, 30, 40, 50, 60, 75, 90, 120, 150, 180, 210, 240, 260, 280, 300, 360, and 420 min, while the standard sampling proposed in literature ($SS\text{-}MTT$) [10], starting from meal ingestion, is t = 0, 10, 20, 30, 60, 90, 120, 150, 180, 240, 300 min. Intravenous lines were then removed, and the subject had lunch immediately after the end of the study ($\sim 1600 \div 1700$), and then a supper ($\sim 2000 \div 2030$).
Average glucose, C-peptide and insulin concentrations are shown in Fig. 4.1.

Analytical techniques. All blood samples were immediately placed on ice, centrifuged at 4°C, separated, and stored at -20°C until assay. Plasma glucose concentrations were measured using a glucose oxidase method (YSI, Yellow Springs, OH). Plasma insulin concentrations were measured by a chemiluminescence assay with reagents (Access Assay; Beckman, Chaska, MN). Plasma C-peptide concentrations were measured by radioimmunoassay (Linco Research, St. Louis, MO). Body composition was measured using

dual-energy X-ray absorptiometry (DPX scanner; Lunar, Madison, WI). Visceral fat was measured by a single-slice computerized tomographic scan at the level of L2/L3 [34]. This standard procedure was adopted for all the databases described in this chapter.

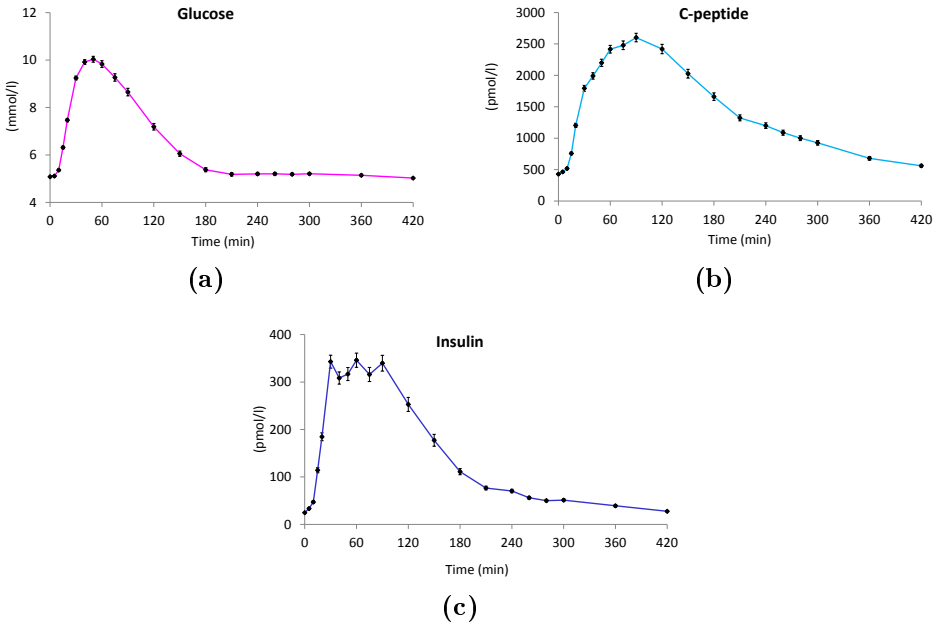

Figure 4.1: Average plasma glucose (a), C-peptide (b), and insulin (c) concentrations, in *database 1* (vertical bars represent ± SE).

4.3 Database 2: prediabetic subjects

Subjects. 32 subjects (17 women and 15 men) with IFG and 28 subjects (17 women and 11 men) with NFG participated in the study [8]. All subjects were Caucasian, in good health, at a stable weight, and not involved in regular vigorous physical exercise. At the time of study, subjects were on no medications except for a stable dose of thyroid hormone, low-dose aspirin, hydroxymethylglutaryl-CoA reductase inhibitors, selective serotonin reuptake inhibitor antidepressants, or antihypertensives, which are considered

metabolically neutral (e.g., no ACE inhibitors or beta-blockers).
All subjects followed a weight-maintenance diet containing 55% carbohydrate, 30% fat, and 15% protein for at least 3 days before the beginning of the study. Fasting plasma glucose concentration was measured after an overnight fast on two separate occasions, at least 1 week apart, in order to classify the subjects: subjects with average fasting glucose level < 5.2 mmol/l or between 5.6 and 7.0 mmol/l were selected for the study as NFG or IFG, respectively. Subjects with fasting glucose between 5.2 and 5.6 mmol/l were excluded, since despite having normal glucose concentrations, it has been demonstrated ([19, 40, 54]) that these individuals have an $\sim$8% risk of developing diabetes within the next 10 years and can thus be considered an early form of IFG.
The selected subjects were admitted to the Mayo CRU on two subsequent occasions at 1700 the evening before the study and ate a standard 10 kcal/kg meal (55% carbohydrate, 30% fat, and 15% protein) between 1830 and 1900. No additional food was eaten until the next morning.

OGTT protocol. On one occasion, subjects ingested 75 g glucose after a 12-h overnight fast. Blood was sampled at t = -30, -20, -10, 0, 10, 15, 20, 30, 45, 60, 75, 90, 120, 150, 180, 210, 240 min. Average glucose, C-peptide and insulin concentrations are shown in Fig. 4.2.
According to these test results, subjects with either NFG or IFG were subclassified as NFG/NGT (2-h plasma glucose < 7.8 mmol/l), NFG/IGT (2-h plasma glucose between 7.8 and 11.1 mmol/l), IFG/IGT, or IFG/diabetes (2-h plasma glucose > 11.1 mmol/l).

Mixed meal protocol. On a further occasion, subjects ingested a labeled mixed meal, as described above, according to [5]. Blood samples were collected at t = -30, -20, -10, 0, 5, 10, 15, 20, 30, 40, 50, 60, 75, 90, 120, 150, 180, 210, 240, 260, 280, 300, 360 min. Average glucose, C-peptide and insulin concentrations are shown in Fig. 4.3.

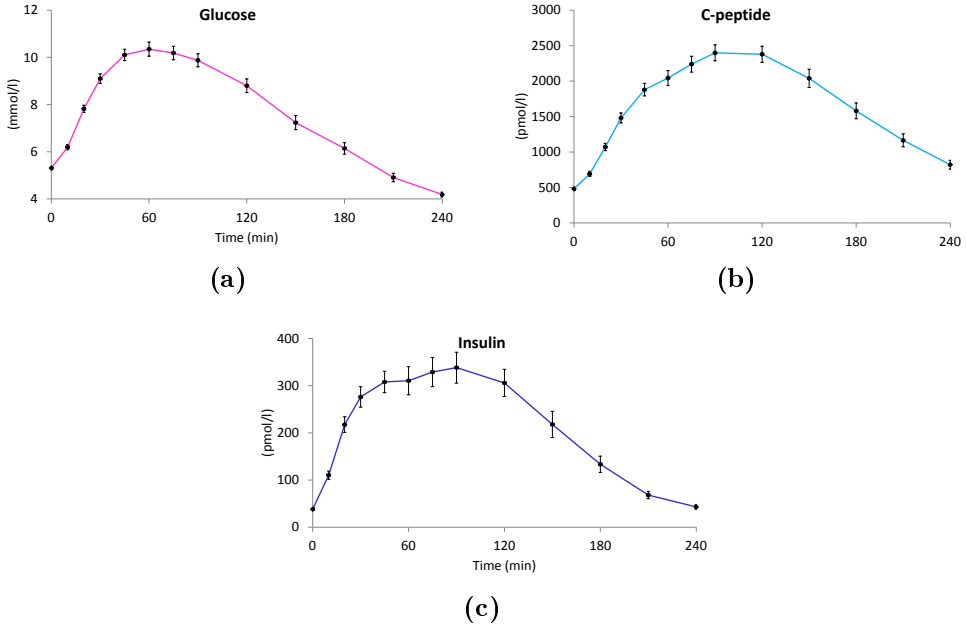

Figure 4.2: OGTT average plasma glucose (a), C-peptide (b), and insulin (c) concentrations, in *database 2* (vertical bars represent ± SE).

4.4 Database 3: healthy and T2DM subjects

Subjects. 14 T2DM and 11 healthy subjects participated in the study [4]; all they were in good health, and not regularly engaged in vigorous physical exercise. Oral antihyperglycemic medications were discontinued 3 weeks before the study. Two diabetic subjects and one non-diabetic subject were receiving thyroxine replacement therapy but had normal thyroidstimulating hormone levels. As usually, all participants had to follow a weight maintenance diet for 3 days before the study. At screening, body composition and visceral fat were measured using dual-energy X-ray absorptiometry and a single-cut computed tomographic scan.

Mixed meal protocol. Also in this case, subjects ingested a labeled mixed meal, as described above and represented in [5]. Blood samples were collected at t = -180, -30, 0, 5, 10, 15, 20, 30, 40, 50, 60, 75, 90, 120, 150, 180,

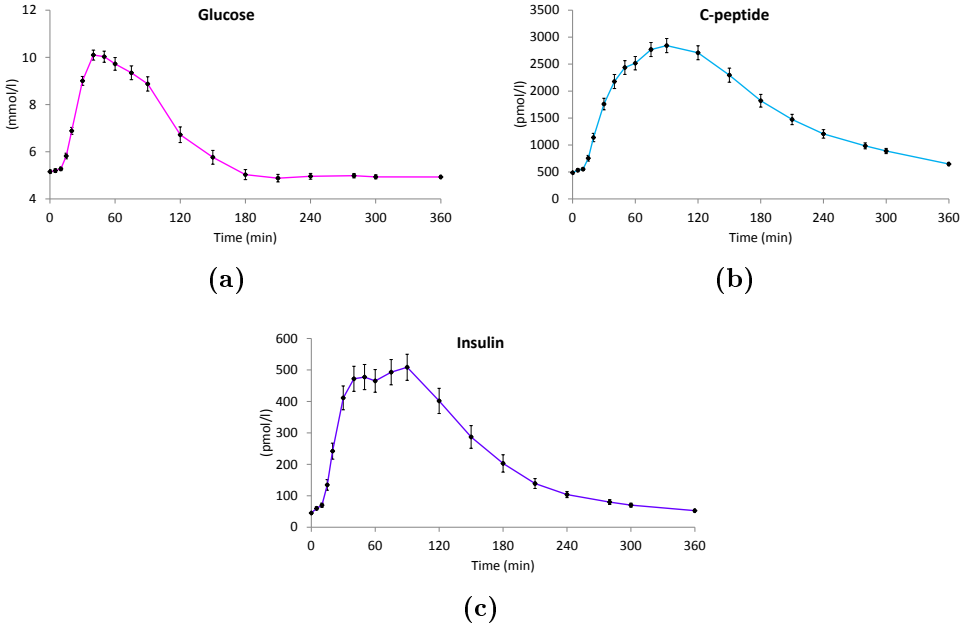

Figure 4.3: Mixed meal average plasma glucose (a), C-peptide (b), and insulin (c) concentrations, in *database 2* (vertical bars represent ± SE).

210, 240, 260, 280, 300, 360 min. Average glucose, C-peptide and insulin concentrations are shown in Fig. 4.4, both for healthy and T2DM subjects.

4.5 Database 4: T2DM subjects

Subjects. 14 subjects with T2DM participated in this study [16]. All they were in good health, stable weight, not engaged in regular vigorous physical exercise, and were not treated with medication altering gastric emptying; moreover, they did not have a history of microvascular complications of diabetes. During the period of the study, the subjects followed the usual weight-maintenance diet.

Mixed meal protocol. A randomized, double-blind, placebo-controlled crossover design was utilized: subjects received either 50 mg vildagliptin or

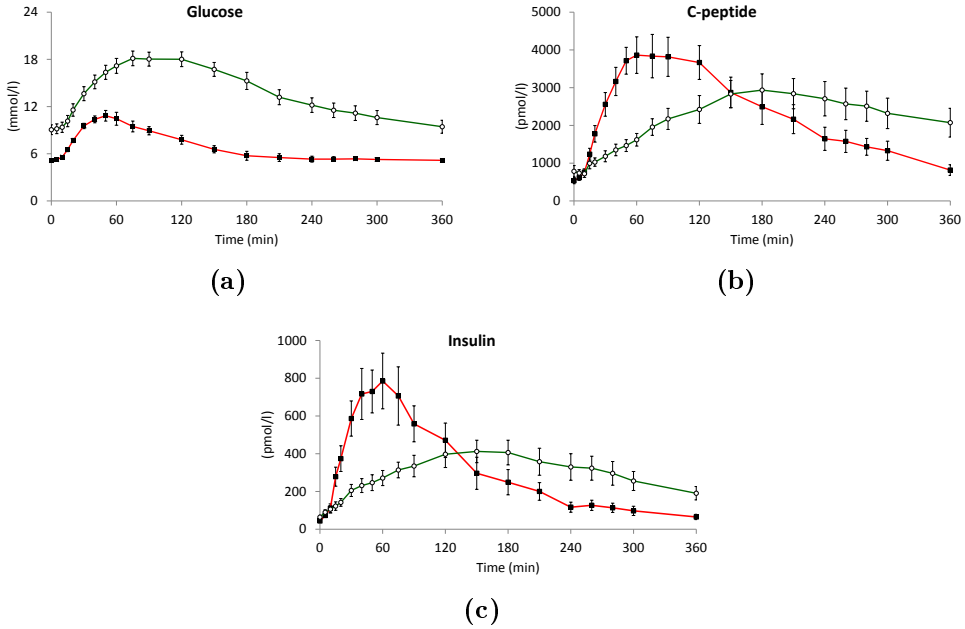

Figure 4.4: Average plasma glucose (a), C-peptide (b), and insulin (c) concentrations, of healthy (■) and T2DM subjects (◯), in *database 3* (vertical bars represent ± SE).

placebo in random order, taken before breakfast and the evening meal over 10 days, in which the two treatments were separated by at least a 2-week washout period.

Subjects were admitted to the Mayo CRU after 6 days of treatment, in the evening. Gastric accommodation was measured on the 7^{th} day of the treatment period. Glucose, insulin, and C-peptide concentrations were collected before and after the ingestion of a mixed meal on day 9.

After an 8-h fast, a forearm vein was cannulated with an 18-gauge needle to the infusions. An 18-gauge cannula was inserted retrogradely into a vein of the dorsum of the opposite hand. This was placed in a heated Plexiglas box maintained at 55° C to allow sampling of arterialized venous blood. At t = -180 min a primed continuous infusion of [6,6-$^2H_2$]glucose was initiated. Subjects received a morning dose consisting of 50 mg vildagliptin or placebo at t = -30 min. At time 0 subjects consumed a meal consisting of two scrambled eggs labeled with 0.75 mCi 99mTc-sulfur colloid, 55g of Canadian bacon, 240

ml of water, and Jell-O containing 75 g glucose labeled with [1-^{13}C]glucose (4% enrichment). This provided 510 kcal (61% carbohydrate, 19% protein, and 21% fat). Blood was sampled at t = -180, -30, -20, -10, 0, 10, 20, 30, 45, 60, 75, 90, 120, 150, 180, 210, 240, 270, 300, 302, 305, 306, 308, 311, 315, 330, 345, 360 min; the average glucose, C-peptide and insulin data are shown in Fig. 4.5, both in presence and absence of vildagliptin. To allow a model-independent assessment of the effect of vildagliptin on insulin action, 5 hours after the start of the study (300 min) subjects received 0.02 unit/kg body weight of insulin intravenously (over a 5-min period) [16].

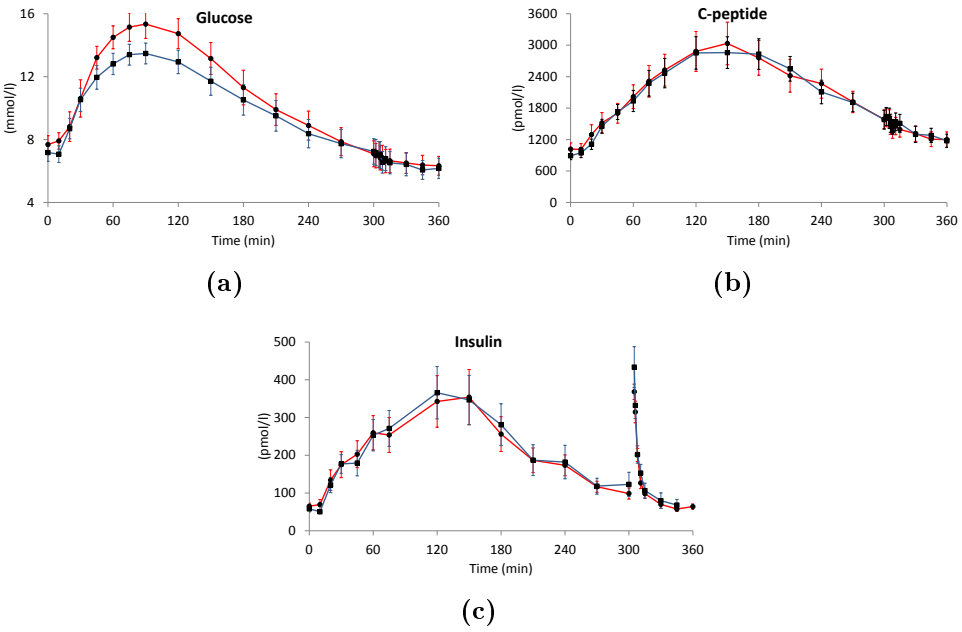

Figure 4.5: Average plasma glucose (a), C-peptide (b), and insulin (c) concentrations, in presence of vildagliptin (■), and in presence of placebo (◯), in *database 4* (vertical bars represent ± SE).

5 Insulin kinetic and HE models

5.1 Introduction

In this chapter, seven models of insulin kinetics and hepatic extraction are proposed; they include an increasing number of compartments and different novel mechanistic descriptions of HE, each taking into account the influence of one or more different modifiers, such as plasma glucose and insulin concentrations.

5.2 Insulin kinetic models

Model 1. This model assumes that insulin kinetics is described by a linear single compartment (see Fig. 5.1, *top* panel), according to the *Model of Data* [11] described in chapter 3:

$$\dot{I}(t) = -n \cdot I(t) + IDR(t)/V_I \tag{5.1}$$

Indexes of HE can easily be obtained: for HE_b and HE_{tot} Eq. (3.36) and (3.35) are used.

Model 2. This model assumes a two-compartment description of insulin kinetics (see Fig. 5.1, *middle* panel), similarly to what reported in [26], and

later in [17]:

$$\dot{I}_L(t) = -[m_1 + m_3(t)] \cdot I_L(t) + m_2 \cdot I_P(t) + \frac{ISR(t)}{(V_P \cdot BW)} \qquad I_L(0) = I_{Lb} \tag{5.2}$$

$$\dot{I}_P(t) = -(m_2 + m_4) \cdot I_P(t) + m_1 \cdot I_L(t) \qquad I_P(0) = I_{Pb} \tag{5.3}$$

$$I(t) = I_P(t) \tag{5.4}$$

where I_L, I_P (pmol/l) are insulin concentrations in liver and plasma, respectively; I (pmol/l) is measured plasma insulin concentration; ISR (pmol/min) is insulin secretion rate; V_P is the volume of insulin distribution (l/kg); m_1, m_2, m_4, (min^{-1}) are rate parameters; m_3 (min^{-1}) is a time-varying parameter which, as in [17], is:

$$m_3(t) = \frac{HE(t) \cdot m_1}{1 - HE(t)} \tag{5.5}$$

According to Eq. (5.2)-(5.3), in basal state, one has:

$$I_{Lb} = \frac{m_2 \cdot I_{Pb} + ISR_b/(BW \cdot V_P)}{m_1 + m_3(0)} \tag{5.6}$$

$$I_{Pb} = I_b \tag{5.7}$$

where:

$$m_3(0) = \frac{HE_b \cdot m_1}{1 - HE_b} \tag{5.8}$$

HE_b can be calculated from Eq. (5.3), using the steady state constraints:

$$HE_b = \frac{ISR_b/(BW \cdot V_P) - m_4 \cdot I_{Pb}}{ISR_b/(BW \cdot V_P) + m_2 \cdot I_{Pb}} \tag{5.9}$$

while HE_{tot} is defined from Eq. (5.5) as follows:

$$HE_{tot} = \frac{\int_0^T m_3(t)dt}{\int_0^T (m_3(t) + m_1)dt} \tag{5.10}$$

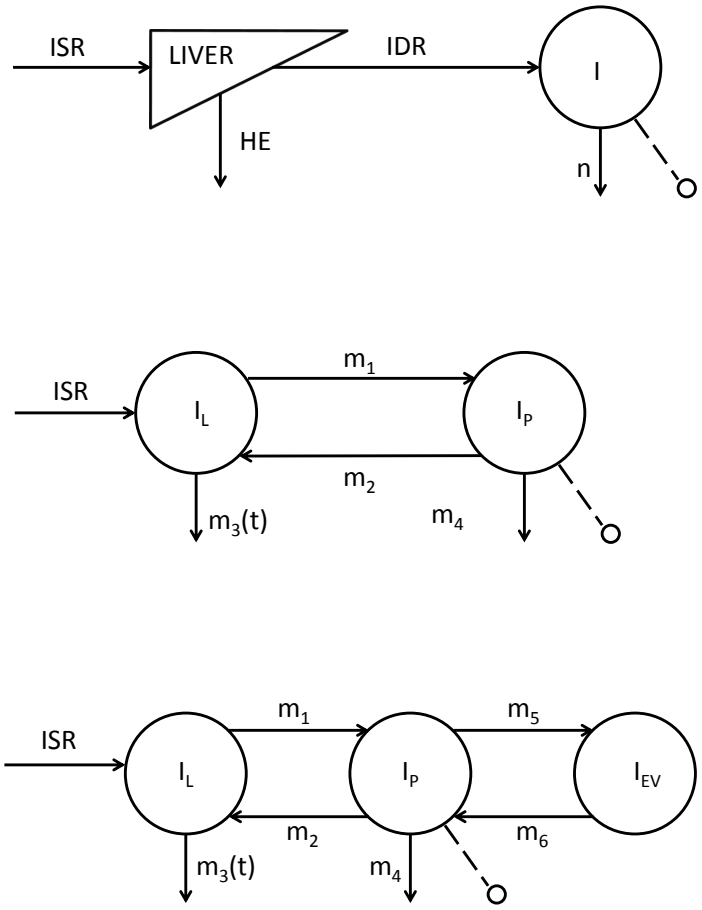

Figure 5.1: Model 1 (*top* panel), Model 2 (*middle* panel), Model 3 (*bottom* panel). I (pmol/l), plasma insulin concentration, accessible to measurement; n (min^{-1}), fractional insulin clearance rate; ISR (pmol/min), insulin secretion rate; IDR (pmol/min), posthepatic insulin delivery rate; I_L, I_P and I_{EV} (pmol/l), insulin concentrations in the liver, plasma and extravascular space, respectively; m_1, m_2, m_4, m_5, m_6 (min^{-1}), rate parameters; m_3 (min^{-1}), time-varying parameter dependent on hepatic insulin extraction HE (%).

Model 3. This model assumes a more physiological three-compartment description of insulin kinetics (see Fig. 5.1, *bottom* panel) across the liver,

plasma and extra-vascular space, according to [44]:

$$\dot{I}_L(t) = -[m_1 + m_3(t)] \cdot I_L(t) + m_2 \cdot I_P(t) + \frac{ISR(t)}{(V_P \cdot BW)} \qquad I_L(0) = I_{Lb} \tag{5.11}$$

$$\dot{I}_P(t) = -(m_2 + m_4 + m_5) \cdot I_P(t) + m_1 \cdot I_L(t) + m_6 \cdot I_{EV}(t) \qquad I_P(0) = I_{Pb} \tag{5.12}$$

$$\dot{I}_{EV}(t) = -m_6 \cdot I_{EV}(t) + m_5 \cdot I_P(t) \qquad I_{EV}(0) = I_{EVb} \tag{5.13}$$

$$I(t) = I_p(t) \tag{5.14}$$

where, compared to *Model 2*, I_{EV} (pmol/l), i.e. insulin concentration in the extra-vascular space, as well as the rate parameters m_5 and m_6 (min^{-1}), have been added.
Eq. (5.5)÷(5.8) from *Model 2* are still valid, and for I_{EV}, in basal state, one has:

$$I_{EVb} = \frac{m_5}{m_6} \cdot I_{Pb} \tag{5.15}$$

For HE_b and HE_{tot} the same formulations shown in Eq. (5.9)-(5.10) hold.

5.3 HE models

As explained in chapter 3, HE has been described by Campioni et al. as a piecewise linear function [11] during a meal tolerance test. This is a *Model of Data* which allows reconstruction of the HE profile from plasma C-peptide, insulin and glucose concentrations and provides an index of overall hepatic extraction, without assuming any mechanistic description of the phenomena controlling hepatic function.

Once its profile is reconstructed, it is easy to observe that, during an oral test, HE decreases when glucose and insulin concentrations rise (see Fig. 4 in [11]). Prior observations suggest that nutrient intake modifies hepatic

extraction of insulin [31, 41], and glucose ingestion both stimulates insulin secretion and reduces hepatic fractional extraction [21]. While this was initially attributed to incretin signaling by the gut, this does not seem to be the case [39]. Indeed, Pivarova et al. [42] have demonstrated that insulin degrading enzyme (IDE) activity is inhibited by hyperglycemia and hyperinsulinemia. Therefore, we attempted to describe HE as a linear function of plasma glucose and insulin alone, and combined.

Here, three different HE descriptions are proposed, each taking into account the influence of one or more different modifiers: plasma glucose and insulin concentrations alone, as well as in combination.

Model a. This model assumes HE to be linearly dependent on plasma glucose concentration G (mmol/l):

$$HE(t) = -a_G \cdot G(t) + a_{0G} \quad HE(0) = HE_b \tag{5.16}$$

where a_G (l/mmol) is a parameter representing the control of plasma glucose on hepatic insulin extraction, and a_{0G} (dimensionless) is obtained from the steady state constraint:

$$a_{0G} = HE_b + a_G \cdot G_b \tag{5.17}$$

An index accounting for glucose control on HE can be derived from the model parameters; in fact, it easy to define the sensitivity of HE to glucose concentration S_G^{HE} (l/mmol) as follows:

$$S_G^{HE} = -\frac{\partial HE(t)}{\partial G}\bigg|_{SS} = a_G \tag{5.18}$$

Model b. This model assumes HE to be dependent on plasma insulin concentration I (pmol/l):

$$HE(t) = -a_I \cdot I(t) + a_{0I} \quad HE(0) = HE_b \tag{5.19}$$

where a_I (l/pmol) is a parameter representing the control of insulin on HE, and a_{0I} (dimensionless) is obtained from the steady state constraint:

$$a_{0I} = HE_b + a_I \cdot I_b \tag{5.20}$$

In this case, an index describing HE sensitivity to insulin, i.e. S_I^{HE}, can be derived:

$$S_I^{HE} = -\frac{\partial HE(t)}{\partial I}\bigg|_{SS} = a_I \tag{5.21}$$

Model c. This model assumes HE to be dependent on both plasma insulin and glucose concentrations:

$$HE(t) = -a_G \cdot G(t) - a_I \cdot I(t) + a_{0GI} \quad HE(0) = HE_b \tag{5.22}$$

where a_{0GI} (dimensionless) is easily obtained from:

$$a_{0GI} = HE_b + a_G \cdot G_b + a_I \cdot I_b \tag{5.23}$$

S_G^{HE} and S_I^{HE} are derived using Eq. (5.18)-(5.21).

5.4 Models of System

Combining the insulin kinetic models listed in paragraph 5.2 with every HE description provided in paragraph 5.3, it would be possible to obtain nine different *Models of System*. However, the HE description corresponding to *Model c* is presented here only for the single-compartment insulin kinetics, since, as highlighted later in chapter 6, this HE formulation makes the model unable to adequately estimate insulin parameters, most likely because of the similarity between glucose and insulin oral trends, which makes numerical identification of the model difficult. That is why here just seven models are presented:

1. **Model I**, obtained from *Model 1* of insulin kinetics and *Model a* of HE (see Fig. 5.2, *top* panel).

2. **Model II**, obtained from *Model 1* of insulin kinetics and *Model b* of HE (see Fig. 5.2, *middle* panel).

3. **Model III**, obtained from *Model 1* of insulin kinetics and *Model c* of HE (see Fig. 5.2, *bottom* panel).

4. **Model IV**, obtained from *Model 2* of insulin kinetics and *Model a* of HE (see Fig. 5.3, *top* panel).

5. **Model V**, obtained from *Model 2* of insulin kinetics and *Model b* of HE (see Fig. 5.3, *bottom* panel).

6. **Model VI**, obtained from *Model 3* of insulin kinetics and *Model a* of HE (see Fig. 5.4, *top* panel).

7. **Model VII**, obtained from *Model 3* of insulin kinetics and *Model b* of HE (see Fig. 5.4, *bottom* panel).

For C-peptide secretion and kinetics, the model described at the beginning of paragraph 3.2.2 [10, 24] is used, thus, both C-peptide and insulin data are predicted simultaneously.

In Table 5.1, the main features of the insulin models (number of compartments, HE descriptions and indexes) are summarized, for readers convenience.

5.5 Model identification

5.5.1 A priori identifiability

All the proposed models are globally identifiable, if the parameter m_2 is assumed to be known in *Models IV, V, VI, VII*, according to DAISY software [7].Parameter m_2 becomes identifiable when an external input enters the

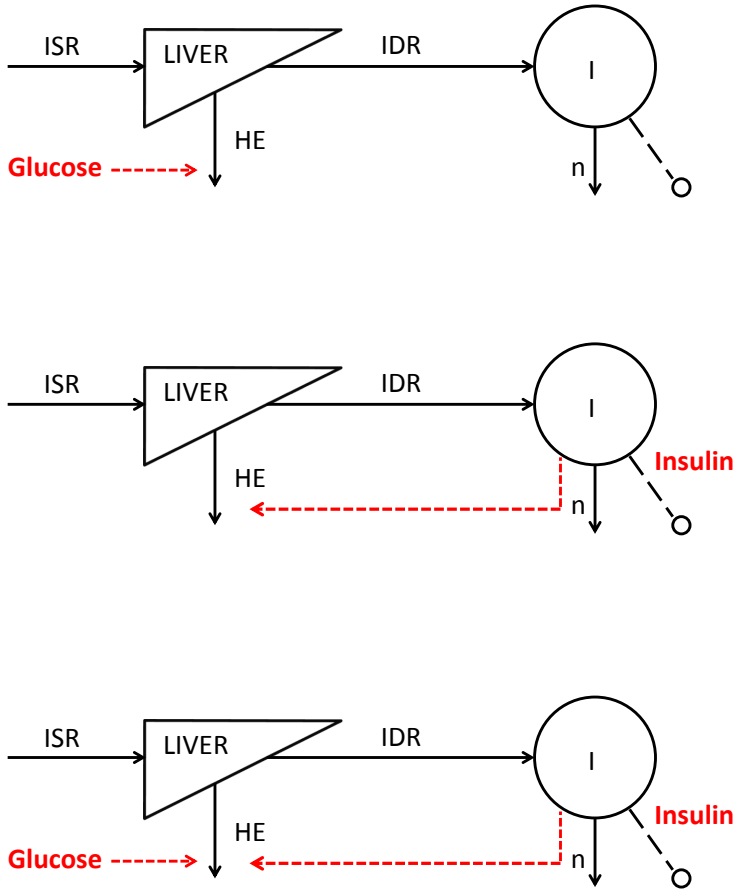

Figure 5.2: Model I (*top* panel), Model II (*middle* panel), Model III (*bottom* panel).

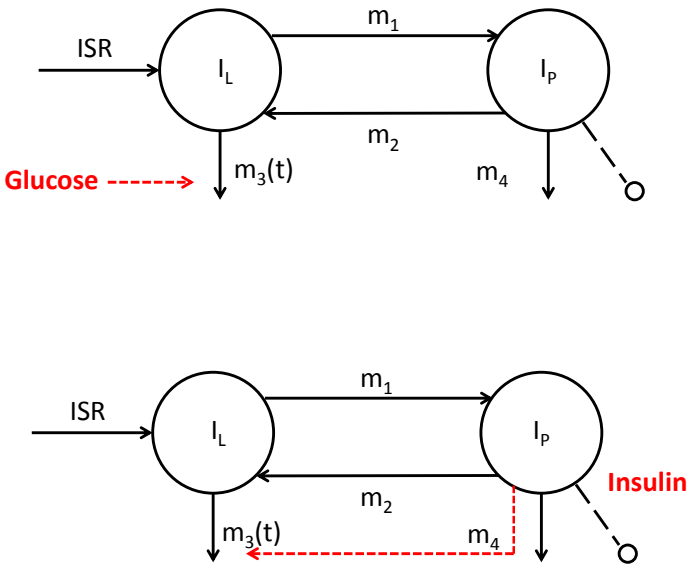

Figure 5.3: Model IV (*top* panel), Model V (*bottom* panel).

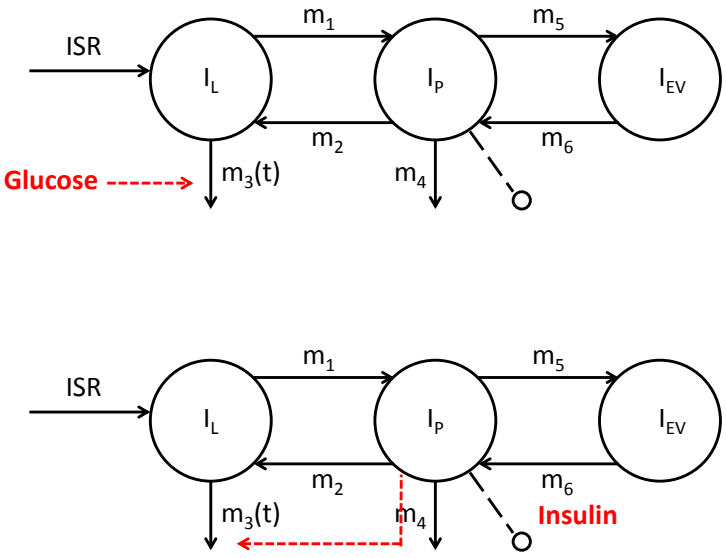

Figure 5.4: Model VI (*top* panel), Model VII (*bottom* panel).

Table 5.1: Number of compartments, HE descriptions and indexes, for each insulin kinetic model.

	N° of compartments	**HE(t)**	$\mathbf{HE_b}$	$\mathbf{HE_{tot}}$	$\mathbf{S_G^{HE}}$	$\mathbf{S_I^{HE}}$
Model of Data	1	$\begin{cases} HE_{i-1} + \frac{HE_i - HE_{i-1}}{(t_i - t_{i-1})} \cdot (t - t_i) \\ HE_0 = HE_b \end{cases}$	$\frac{ISR_b - IDR_b}{ISR_b}$	$\frac{\int_0^T ISR(t)dt - \int_0^T IDR(t)dt}{\int_0^T ISR(t)dt}$	N.A.	N.A.
Model I	1	$-a_G \cdot G(t) + a_{0G}$	$\frac{ISR_b - IDR_b}{ISR_b}$	$\frac{\int_0^T ISR(t)dt - \int_0^T IDR(t)dt}{\int_0^T ISR(t)dt}$	a_G	N.A.
Model II	1	$-a_I \cdot I(t) + a_{0I}$	$\frac{ISR_b - IDR_b}{ISR_b}$	$\frac{\int_0^T ISR(t)dt - \int_0^T IDR(t)dt}{\int_0^T ISR(t)dt}$	N.A.	a_I
Model III	1	$-a_G \cdot G(t) - a_I \cdot I(t) + a_{0GI}$	$\frac{ISR_b - IDR_b}{ISR_b}$	$\frac{\int_0^T ISR(t)dt - \int_0^T IDR(t)dt}{\int_0^T ISR(t)dt}$	a_G	a_I
Model IV	2	$-a_G \cdot G(t) + a_{0G}$	$\frac{ISR_b/(BW \cdot V_P) - m_4 \cdot I_{Pb}}{ISR_b/(BW \cdot V_P) + m_2 \cdot I_{Pb}}$	$\frac{\int_0^T m_3(t)dt}{\int_0^T (m_3(t) + m_1)dt}$	a_G	N.A.
Model V	2	$-a_I \cdot I(t) + a_{0I}$	$\frac{ISR_b/(BW \cdot V_P) - m_4 \cdot I_{Pb}}{ISR_b/(BW \cdot V_P) + m_2 \cdot I_{Pb}}$	$\frac{\int_0^T m_3(t)dt}{\int_0^T (m_3(t) + m_1)dt}$	N.A.	a_I
Model VI	3	$-a_G \cdot G(t) + a_{0G}$	$\frac{ISR_b/(BW \cdot V_P) - m_4 \cdot I_{Pb}}{ISR_b/(BW \cdot V_P) + m_2 \cdot I_{Pb}}$	$\frac{\int_0^T m_3(t)dt}{\int_0^T (m_3(t) + m_1)dt}$	a_G	N.A.
Model VII	3	$-a_I \cdot I(t) + a_{0I}$	$\frac{ISR_b/(BW \cdot V_P) - m_4 \cdot I_{Pb}}{ISR_b/(BW \cdot V_P) + m_2 \cdot I_{Pb}}$	$\frac{\int_0^T m_3(t)dt}{\int_0^T (m_3(t) + m_1)dt}$	N.A.	a_I

plasma insulin compartment (see par. 7.4).
DAISY is a computer tool, implementing a differential algebra algorithm used to automatically perform the parameter identifiability analysis, both for linear and nonlinear dynamic models, described by differential equations. In this case, it was particularly useful because of the nonlinearity in Eq. (5.5), that made a manual calculation complicated to solve.

5.5.2 Numerical identification

C-peptide and insulin models were identified in all the subjects by nonlinear weighted least squares [13] implemented in Matlab. If some parameters provided a poor estimation precision, a Maximum A Posteriori (MAP) Bayesian estimator approach was adopted. Error on C-peptide and insulin measurements was assumed to be independent, Gaussian, with zero mean and variance dependent to the C-peptide and insulin measurements, respectively, as reported in [50]:

$$var(Cp) = 2000 + 0.001 \cdot Cp^2 \tag{5.24}$$

$$var(I) = 6 + 0.0055 \cdot I^2 \tag{5.25}$$

Glucose is the model forcing function, thus it is assumed to be known without error.

As mentioned in chapter 3, the simultaneous estimation of both secretion and kinetics is possible thanks to the method proposed by Van Cauter [55]: in particular the C-peptide kinetic parameters (k_{01}, k_{21}, k_{12}, V_c) are fixed, according to the following population models:

$$k_{12} = FRA \cdot B1 + (1 - FRA) \cdot A1 \tag{5.26}$$

$$k_{01} = \frac{A1 \cdot B1}{k_{12}} \tag{5.27}$$

$$k_{21} = A1 + B1 - k_{12} - k_{01} \tag{5.28}$$

$$V_c = \begin{cases} BSA \cdot 1.92 + 0.64 & if sex = M \\ BSA \cdot 1.11 + 2.04 & if sex = F \end{cases} \tag{5.29}$$

where:

$$AB = 0.14 \cdot age + 29.16 \tag{5.30}$$

$$B1 = \frac{ln2}{AB} \tag{5.31}$$

$$FRA = \begin{cases} 0.78 & if BMI > 27 \\ 0.76 & if BMI \leq 27 \end{cases} \tag{5.32}$$

$$A1 = \begin{cases} 0.52 & if BMI > 27 \\ 0.14 & if BMI \leq 27 \end{cases} \tag{5.33}$$

For the *Model of Data*, as hinted in chapter 3, Campioni et al. [11] had to develop linear regression models linking CL_I and V_I to anthropometric characteristics, in order to be able to fix V_I and n, and to just estimate the HE breakpoints:

$$ln(V_I) = 0.814 + 0.754 \cdot BSA - 0.000908 \cdot age \tag{5.34}$$

$$ln(CL_I) = -0.0402 + 0.372 \cdot BSA - 0.00313 \cdot age \tag{5.35}$$

Eq. (5.34)-(5.35) were also used for all the other single-compartment insulin kinetic descriptions (*Model I, II, III*).
In *Model IV, V, VI, VII*, all the insulin kinetic parameters are estimated, except for m_2, which is fixed to 0.268 min^{-1}, as suggested in [27], and done in [44].

5.6 Statistical analysis

Data are presented as mean±SD, unless otherwise stated. Pearson's linear correlation was adopted to evaluate univariate correlation. Two samples

paired and unpaired comparisons were undertaken using nonparametric and T-test (depending on the outcome of the gaussianity test of each distribution).

5.7 Model selection

The best model selected among *Model of Data, Model I, Model II, Model of III, Model IV, Model V, Model VI, Model VII*, is chosen by comparing model performances on the basis of different criteria: residual independence (Anderson Run Test), precision of parameters estimates (expressed as percent coefficient of variation, CV%), ability to describe the data (weighted residual square sum, WRSS), and model parsimony (Akaike Information Criterion, AIC), here calculated as follows:

$$AIC = WRSS + 2P \tag{5.36}$$

where P is the number of estimated parameters.

6 Model assessment in database 1

6.1 Introduction

In this chapter, the models are assessed using *database 1*. Results of the simultaneous identification of oral C-peptide minimal model and each insulin kinetic model (*Model of Data, Model I, Model II, Model III, Model IV, Model V, Model VI, Model VII*) are presented. Then, after selecting the optimal model among them, the reconstructed HE profiles and indexes are shown. Finally, a comparison between the frequent and standard sampling condition is provided.

6.2 Model selection

The time courses of weighted residuals, obtained with the previously published *Model of Data* and with the new tested models, are reported in Fig. 6.1÷6.8 (C-peptide and insulin, *top* and *bottom* panel, respectively).

Results of the model comparison are summarized in Table 6.1, both for the C-peptide and insulin sub-models.
Models IV, V have been discarded, because randomness of the insulin weighted residuals is supported by the Run Test in only 59% and 67%, of the cases, respectively, and the estimated parameters, especially those of the C-peptide

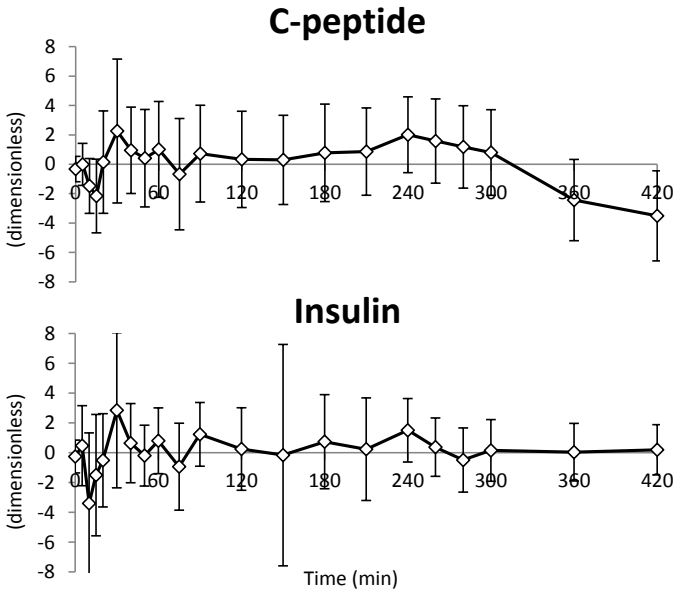

Figure 6.1: Average C-peptide (*top* panel) and insulin (*bottom* panel) weighted residuals for Model of Data (vertical bars represent ± SD).

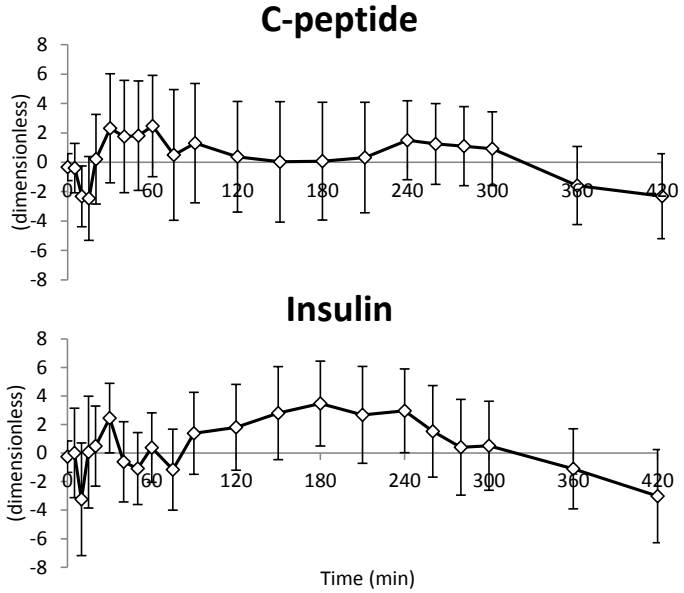

Figure 6.2: Average C-peptide (*top* panel) and insulin (*bottom* panel) weighted residuals for Model I (vertical bars represent ± SD).

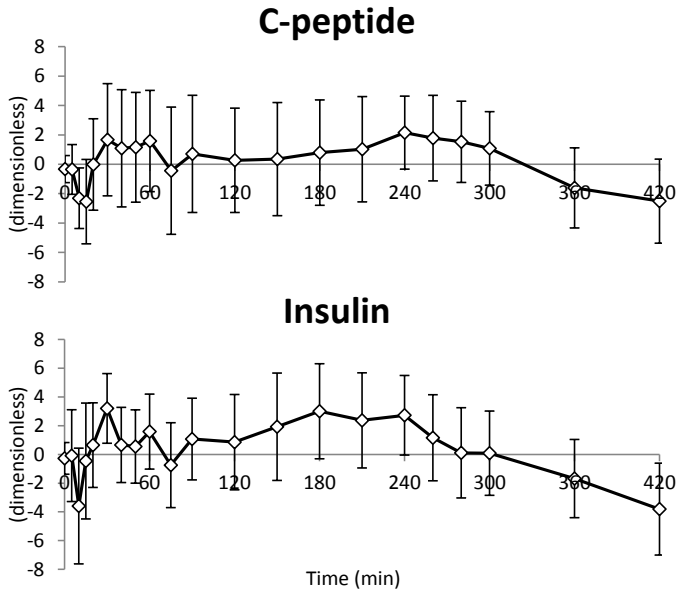

Figure 6.3: Average C-peptide (*top* panel) and insulin (*bottom* panel) weighted residuals for Model of II (vertical bars represent ± SD).

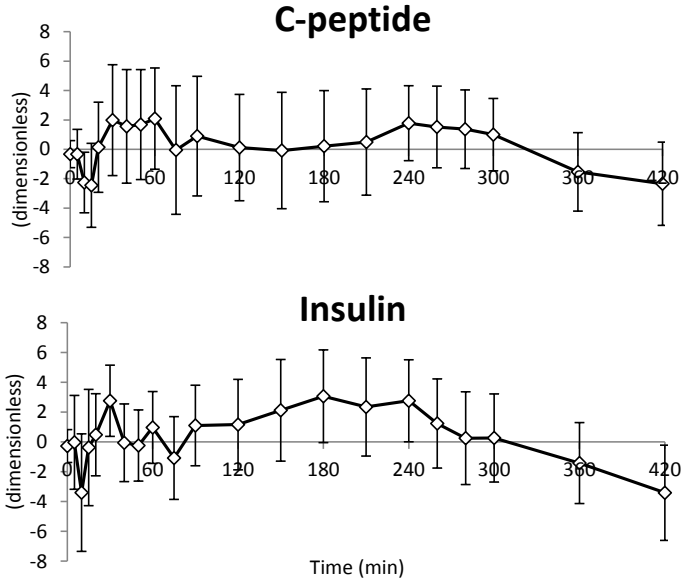

Figure 6.4: Average C-peptide (*top* panel) and insulin (*bottom* panel) weighted residuals for Model III (vertical bars represent ± SD).

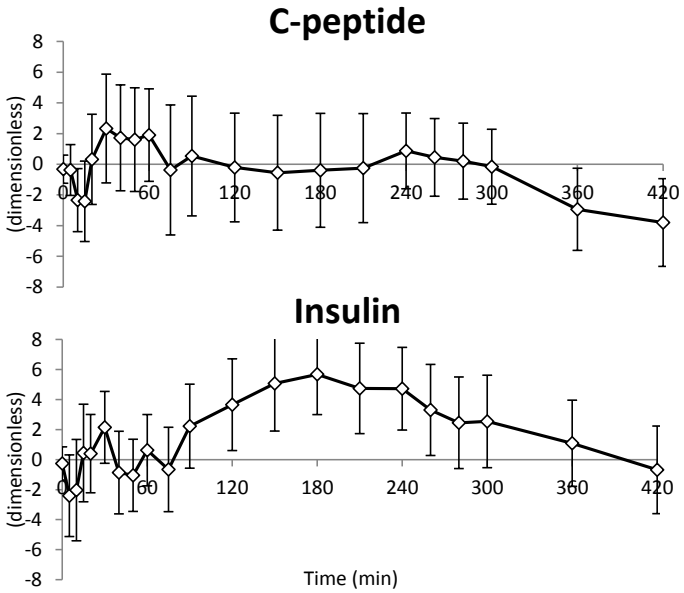

Figure 6.5: Average C-peptide (*top* panel) and insulin (*bottom* panel) weighted residuals for Model IV (vertical bars represent ± SD).

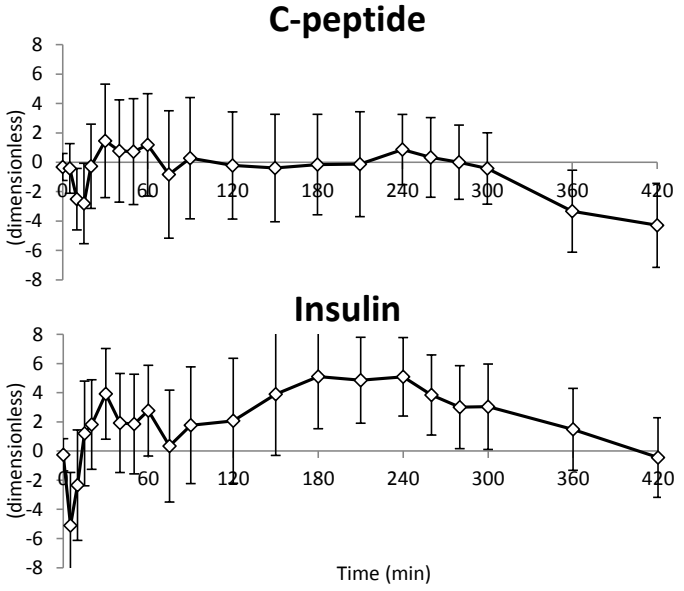

Figure 6.6: Average C-peptide (*top* panel) and insulin (*bottom* panel) weighted residuals for Model V (vertical bars represent ± SD).

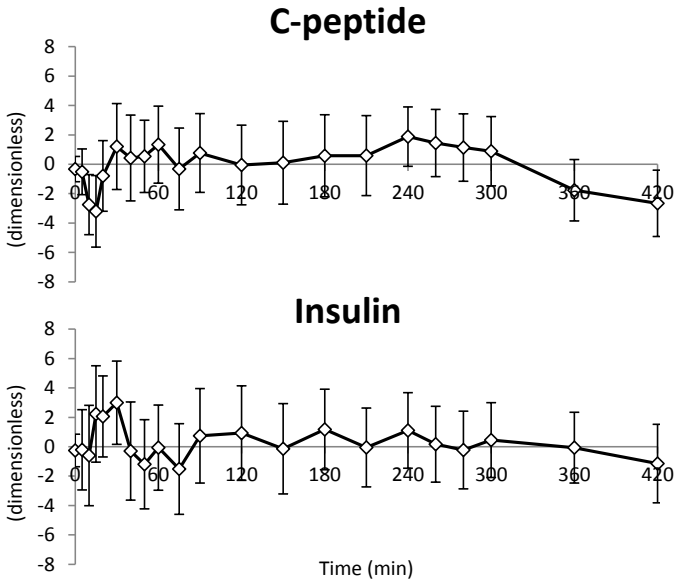

Figure 6.7: Average C-peptide (*top* panel) and insulin (*bottom* panel) weighted residuals for Model VI (vertical bars represent ± SD).

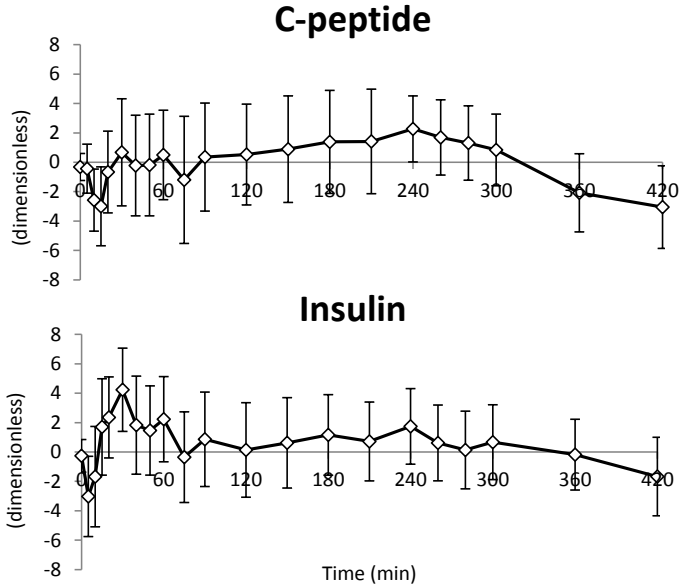

Figure 6.8: Average C-peptide (*top* panel) and insulin (*bottom* panel) weighted residuals for Model VII (vertical bars represent ± SD).

model, show the poor precision (high CV).
Models III, VII were also discarded, because parameters were estimated with poor precision.
For what concerns the remaining models, that are *Model of Data, Models I, II* and *VI*, *Model I* and *Model II* have been discarded since whiteness of weighted residuals was not strongly supported by the Anderson Run Test (see also Fig. 6.2-6.3). *Model of Data* and *Model VI* can fit data and provide good precision of parameter estimates, but AIC index shows that *Model VI* is the most parsimonious ($AIC_{C-peptide}$=156±100 and $AIC_{Insulin}$=136±57), meaning that it provides the best compromise between model complexity and ability to fit the data.
It is of note that, however, the average weighted residuals of *Model VI* are not random at the beginning of the test. C-peptide is slightly over-fitted (see Fig. 6.7, *top* panel), but this also happens with the *Model of Data* (see Fig. 6.1, *top* panel), and thus *Model VI* remains superior, in terms of parsimony. As regards insulin, in t = 15, 20, 30 min, there is a sort of under-fitting, on average (see Fig. 6.7, *bottom* panel), but this is due to a small subset of subjects (approximately 5%).
The parameter estimates and precision provided by the selected model are shown in Table 6.2.

As mentioned above, *Model VI* includes three compartments of insulin kinetics; this particular description is more physiological, when compared to the single and two-compartment models, since it considers plasma, liver and extravascular spaces, as well as the exchange fluxes linking them. In fact, the presence of a second insulin compartment, besides that in plasma, has been initially proposed in [26], and later demonstrated in [25, 47], where insulin first in dogs and then in humans, was assumed to traverse the capillary endothelial barrier in both directions (plasma-interstitial spaces). Thus, in order to provide a realistic description of insulin extraction mediated by the liver, here the chosen model includes a hepatic compartment, as described even in [17], thus adopting the existing three-compartment description of insulin kinetics shown in [44].

Table 6.1: Model selection. Summary results.

	Run Test	**Precision (mean CV)**	**WRSS (mean±SD)**	**Estimated parameters**	**N° of parameters**	**AIC (mean±SD)**
C-peptide						
Model of Data	93%	7%	231±299	α, Φ_d, Φ_s, h	4	239±299
Model I	81%	7%	267±430	α, Φ_d, Φ_s, h	4	275± 430
Model II	87%	7%	255±350	α, Φ_d, Φ_s, h	4	263± 350
Model III	84%	7%	256±343	α, Φ_d, Φ_s, h	4	264±343
Model IV	90%	$>10^4$%	245±319	α, Φ_d, Φ_s, h	4	253±319
Model V	89%	$>10^4$%	253±325	α, Φ_d, Φ_s, h	4	261±325
Model VI	93%	6%	148±100	α, Φ_d, Φ_s, h	4	156±100
Model VII	88%	247%	237±323	α, Φ_d, Φ_s, h	4	245±323
Isulin						
Model of Data	98%	31%	247±664	HE_i (i=1,...,6)	6	259±664
Model I	89%	12%	272±158	a_G	1	274± 158
Model II	91%	10%	268±121	a_I	1	270± 121
Model III	94%	203%	248±117	a_I, a_G	2	252±117
Model IV	59%	96%	329±152	a_G, V_P, m_1, m_4	4	337±152
Model V	67%	5%	427±251	a_I, V_P, m_1, m_4	4	435±251
Model VI	98%	22%	124±57	a_G, V_P, m_1, m_4, m_5, m_6	6	136±57
Model VII	94%	10%	227±164	a_I, V_P, m_1, m_4, m_5, m_6	6	239±164

Table 6.2: Parameter estimates and precision (CV), obtained with Model VI.

Parameters	Units	Estimates (mean±SD)	CV (%)
$\mathbf{V_P}$	(l/kg)	0.057±0.021	30
$\mathbf{a_G}$	(l/mmol)	0.144±0.064	15
$\mathbf{m_4}$	($\min^{-1}$)	0.335±0.178	14
$\mathbf{m_5}$	($\min^{-1}$)	0.283±0.116	20
$\mathbf{m_6}$	($\min^{-1}$)	0.018±0.008	21
$\mathbf{m_1}$	($\min^{-1}$)	0.946±0.424	34
$\boldsymbol{\alpha}$	($\min^{-1}$)	0.091±0.085	11
$\mathbf{\Phi_d}$	(10^{-9})	558.3±236.0	7
$\mathbf{\Phi_s}$	(10^{-9} $\min^{-1}$)	34.24±12.50	3
$\mathbf{h}$	(mmol/l)	4.690±0.523	2

6.3 Reconstructed HE profiles

The selected model, i.e., *Model VI*, allows reconstruction of individual HE profiles. The resulting average HE is shown in Fig. 6.9 together with that provided by the *Model of Data*, and thus included in the literature [11]. Evidently, HE decreases more rapidly and to a greater extent with the *Model VI*, than with the *Model of Data*; in addition, the new profile returns to its basal state at the end of the experiment, as would be expected 420 minutes after meal ingestion. This difference can be explained by observing that the HE expression of the *Model of Data* consists of a piecewise linear function with seven breakpoints, which make the model vulnerable to noise. On the other hand, the description of HE proposed in *Model VI* is a linear function of plasma glucose concentration, thus the end-test steady state is guaranteed insofar as plasma concentrations have returned to basal. It is also remarkable that these two profiles are obtained from two completely different models of insulin kinetics, as explained above, which of course yield different HE results.

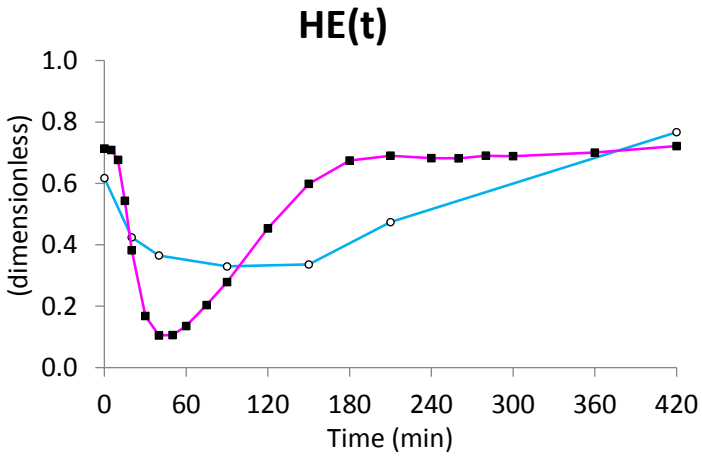

Figure 6.9: Average HE profile of Model of Data (◯) and Model VI (■).

6.4 HE indexes

The basal (HE_b) and total (HE_{tot}) hepatic insulin extraction indexes obtained with *Model VI* [Eq. (5.9)-(5.10)] and with the *Model of Data* [Eq. (3.36)-(3.35)] have been compared. The basal average values differ significantly [$HE_b^{Modelof Data} = 0.617 \pm 0.090$, $HE_b^{ModelVI} = 0.710 \pm 0.109$, $p < 0.0001$; see Fig. 6.10, (a)]. This is due to the fact that, in *Model VI*, HE_b also depends on m_4, that is one of the estimated parameters, while in the *Model of Data*, the same index is calculated from population values and basal measurements. Similarly, the total hepatic extraction index is significantly different in the two cases [$HE_{tot}^{Modelof Data} = 0.435 \pm 0.145$, $HE_{tot}^{ModelVI} = 0.655 \pm 0.139$, $p = 0.0001$; see Fig. 6.10, (b)], as one could expect, since HE_b calculation, the insulin kinetics and the HE descriptions are different, too.
Moreover, it has been assessed whether model derived indexes were different in young (Y) and elderly (E) people, similarly to what reported in [6]. Our results show that HE_b and HE_{tot} did not significantly differ in E compared to Y people [$HE_b = 0.703 \pm 0.116$ vs. 0.728 ± 0.091, $p > 0.05$; $HE_{tot} = 0.646 \pm 0.119$ vs. 0.677 ± 0.146, respectively, $p > 0.05$; see Fig. 6.11, (a), (c), respectively], while S_G^{HE} was significanlty lower in E vs. Y subjects [$S_G^{HE} = 0.136 \pm 0.062$ vs. 0.164 ± 0.065 l/mmol, respectively, $p < 0.05$; see Fig. 6.11,

(e)].

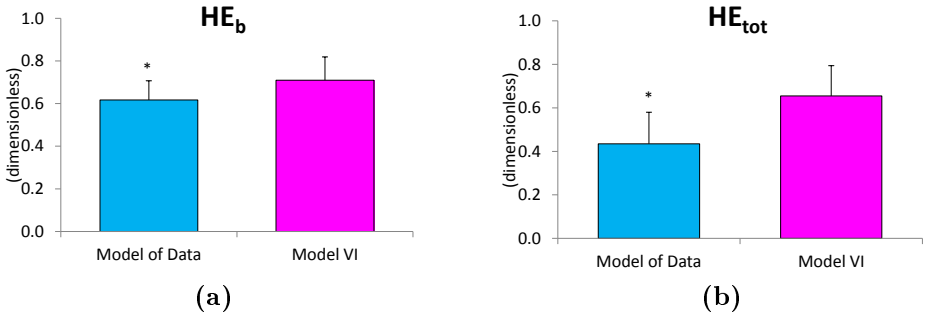

Figure 6.10: HE_b (a) and HE_{tot} (b) indexes, derived from Model of Data, and Model VI. * $p < 0.05$.

6.5 Frequent sampling vs. standard sampling

The new model performed well even if data of a standard [10] (*SS*), instead of a frequently sampled [6] (*FS*), MTT are used (see Fig. 6.12 for the corresponding time grids). Results are shown in Table 6.3. Run Test confirms that *SS* weighted residuals are random in quite all the subjects, and the WRSS values, normalized according to the number of samples (nWRSS), are comparable with those obtained with the *FS-MTT*. Moreover, the precision of parameter estimates is still good, despite the loss of 10 time samples.
HE indexes obtained using the *SS* and *FS-MTT* (see average estimates in Table 6.4) are well correlated, as evident from Fig. 6.13 (R=0.77, p<0.0001 for HE_b; R=0.77, p<0.0001 for HE_{tot}; R = 0.61, p < 0.0001 for S_G^{HE}). Furthermore, S_G^{HE} was still significantly lower in E vs. Y when estimated with the *SS-MTT* [$S_G^{HE} = 0.172 \pm 0.080$ vs. 0.196 ± 0.092 l/mmol, $p < 0.05$; see Fig. 6.11, (f)], while no difference was revealed in HE_b [$HE_b = 0.722 \pm 0.174$ vs. 0.743 ± 0.142, $p > 0.05$; see Fig. 6.11, (b)] and HE_{tot} [$HE_{tot} = 0.641 \pm 0.146$ vs. 0.685 ± 0.119, $p > 0.05$; see Fig. 6.11, (d)], confirming the results provided by the *FS-MTT*.

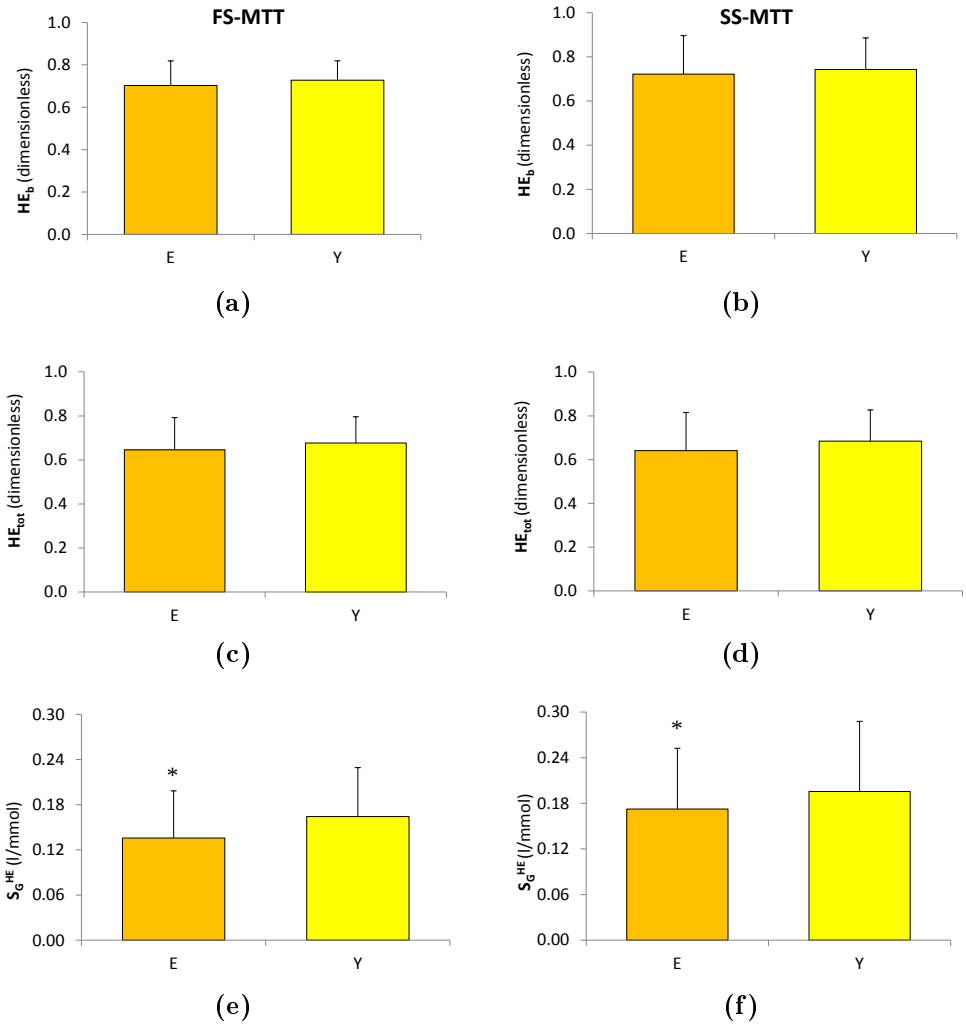

Figure 6.11: Indexes of basal hepatic insulin extraction, HE_b, (a, b), total hepatic insulin extraction, HE_{tot}, (c, d), and hepatic insulin extraction sensitivity to glucose, S_G^{HE}, (e, f), derived from Model VI in elderly and young subjects (E and Y, respectively), using frequent sampling (FS-MTT) (*left*) and standard sampling (SS-MTT) (*right*). * $p < 0.05$.

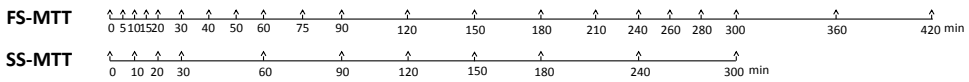

Figure 6.12: *FS-* and *SS-MTT* sampling grids.

Table 6.3: Model VI: comparison between FS and SS-MTT.

	N° of samples	Run Test	Precision (mean CV)	nWRSS (mean±SD)
C-peptide				
FS-MTT	21	93%	6%	7±5
SS-MTT	11	97%	13%	8±14
Insulin				
FS-MTT	21	98%	22%	6±3
SS-MTT	11	97%	27%	5±6

Table 6.4: HE indexes in FS- vs. SS-MTT.

Index	**Units**	**FS-MTT estimates (mean±SD)**	**FS-MTT estimates (mean±SD)**
$\mathbf{HE_b}$	(dimensionless)	0.710±0.109	0.729±0.108
$\mathbf{HE_{tot}}$	(dimensionless)	0.655±0.139	0.655±0.166
$\mathbf{S_G^{HE}}$	(l/mmol)	0.144±0.064	0.180±0.085

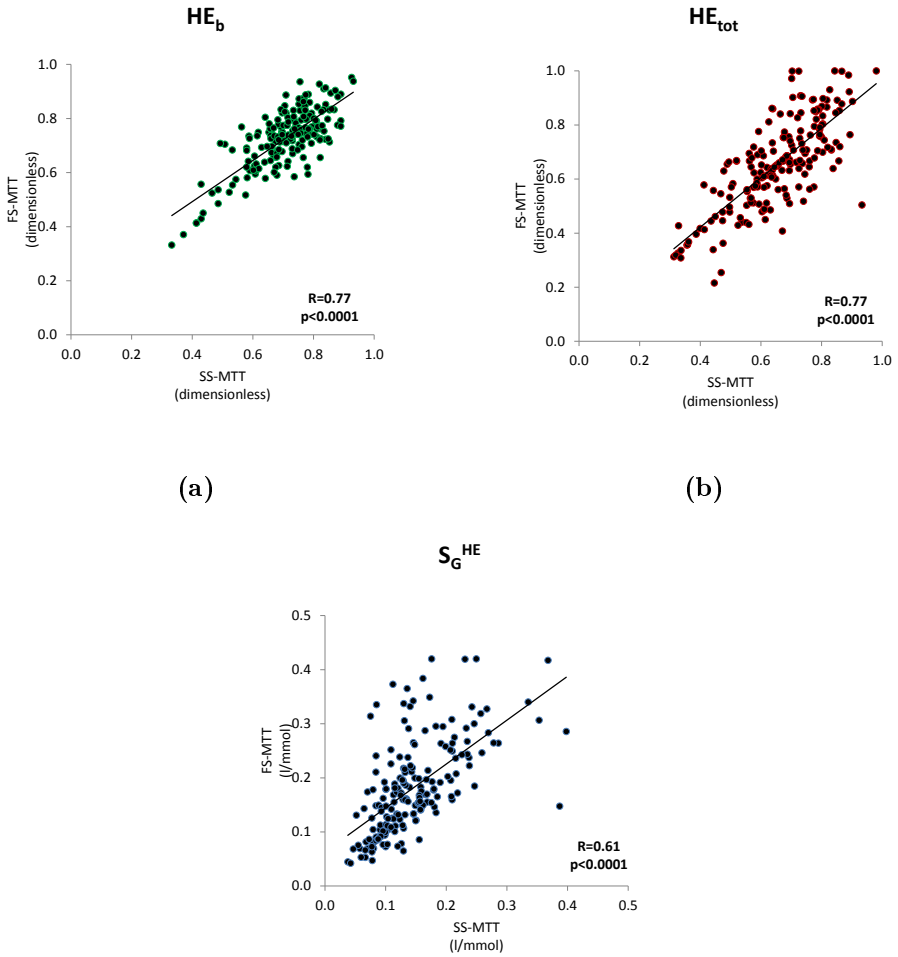

Figure 6.13: HE_b (a), HE_{tot} (b), S_G^{HE} (c) indexes: correlation between the FS and SS-MTT.

7 Model employment

7.1 Introduction

In this chapter *Model VI*, selected in the previous chapter as the most parsimonious one in a database of healthy subjects, is employed to assess its performance in all the spectrum of glucose tolerance. To this purpose, we used *database 2*, made up of prediabetic subjects who underwent both a MTT and an OGTT, *database 3*, made up of healthy and T2DM subjects, and *database 4*, made up of T2DM subjects.

7.2 Database 2

As explained in chapter 4, the prediabetic subjects within *database 2* underwent a MTT, as well as an OGTT. In the following paragraphs, the model performances in both these tests are presented.

7.2.1 Meal

Model VI can well predict both C-peptide and insulin MTT data of *database 2* [8], as evident from the average weighted residuals shown in Fig.

7.1 (C-peptide and insulin, *top* and *bottom* panel, respectively). Moreover, it provides precise estimates of the parameters (see Table 7.1).

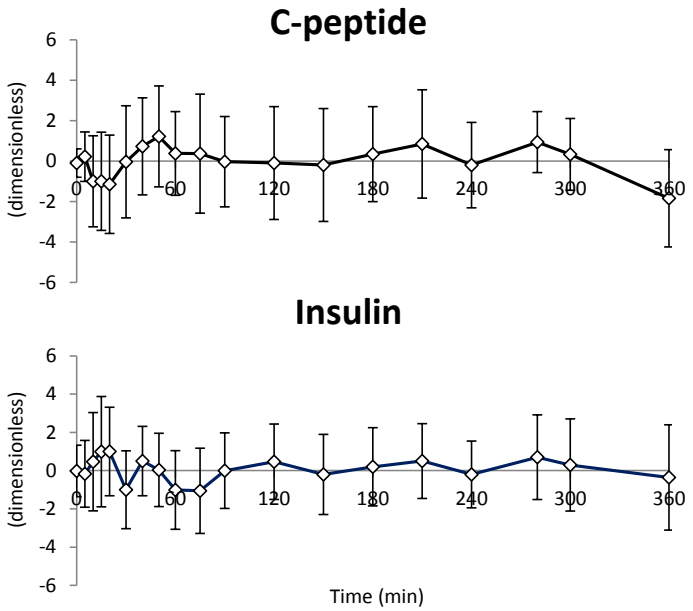

Figure 7.1: Average C-peptide (*top* panel) and insulin (*bottom* panel) weighted residuals, in *database 2*, during meal (vertical bars represent ± SD).

Table 7.1: Parameter estimates and precision (CV), in *database 2*, during meal.

Parameters	**Units**	**Estimates (mean±SD)**	**CV (%)**
$\mathbf{V_P}$	(l/kg)	0.049±0.023	48
$\mathbf{a_G}$	(l/mmol)	0.140±0.069	25
$\mathbf{m_4}$	($\min^{-1}$)	0.333±0.112	18
$\mathbf{m_5}$	($\min^{-1}$)	0.279±0.105	25
$\mathbf{m_6}$	($\min^{-1}$)	0.017±0.010	22
$\mathbf{m_1}$	($\min^{-1}$)	1.229±0.529	54
$\boldsymbol{\alpha}$	($\min^{-1}$)	0.089±0.061	12
$\mathbf{\Phi_d}$	(10^{-9})	625.9±325.3	9
$\mathbf{\Phi_s}$	(10^{-9} $\min^{-1}$)	36.86±13.07	3
$\mathbf{h}$	(mmol/l)	4.733±0.543	4

Another interesting result concerns the difference found in HE profiles and indexes, in NGT (n=25) vs. IFG/IGT (n=16) subjects (see correspond-

ing data in Fig. 7.2). The HE profile is lower in IFG/IGT, on average (Fig. 7.3). The statistical tests confirm that HE_b and HE_{tot} indexes are higher in NGT than IFG/IGT subjects (HE_b = 0.626±0.137 vs. 0.532±0.137, p < 0.05; HE_{tot} = 0.613±0.192 vs. 0.491±0.137, p < 0.05, respectively) (see Fig. 7.4), while no difference is found in S_G^{HE} (S_G^{HE} = 0.155±0.070 vs. 0.140±0.050 l/mmol, p > 0.05, respectively). These results are congruent with the plasma concentration profiles shown in Fig. 7.2, since plasma glucose is higher in IFG/IGT than NGT.

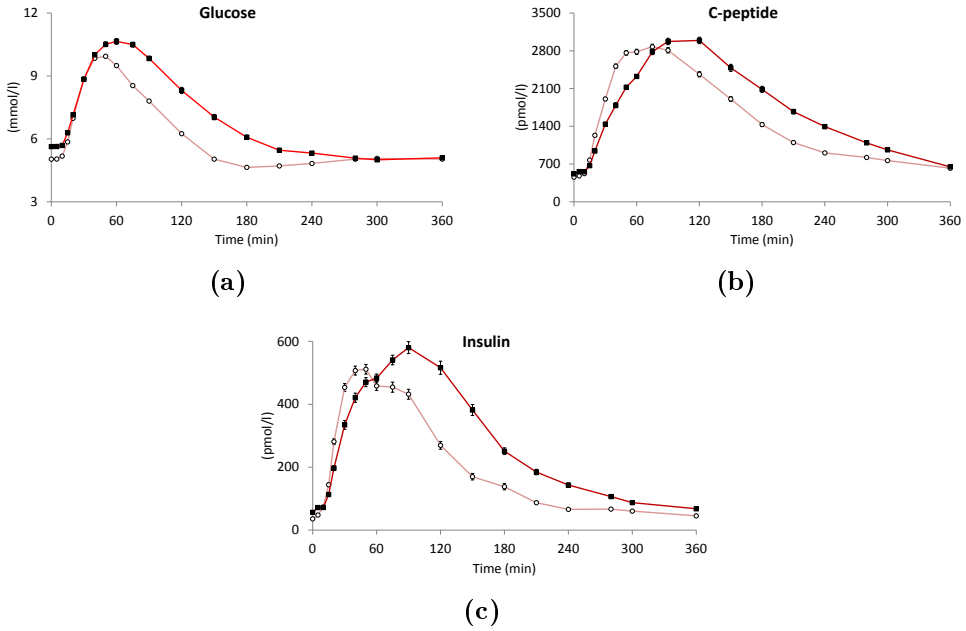

Figure 7.2: Average plasma glucose (a), C-peptide (b), and insulin (c) concentrations of NGT (◯) and IFG/IGT (■) subjects, in *database 2*, during meal (vertical bars represent ± SE).

7.2.2 Oral Glucose Tolerance Test (OGTT)

The model, originally developed for a MTT, has also been used in the OGTT data of the same prediabetic subjects composing *database 2*. As shown by the average weighted residuals plotted in Fig. 7.5, the model can adequately predict C-peptide data, even during the OGTT. Evidently from

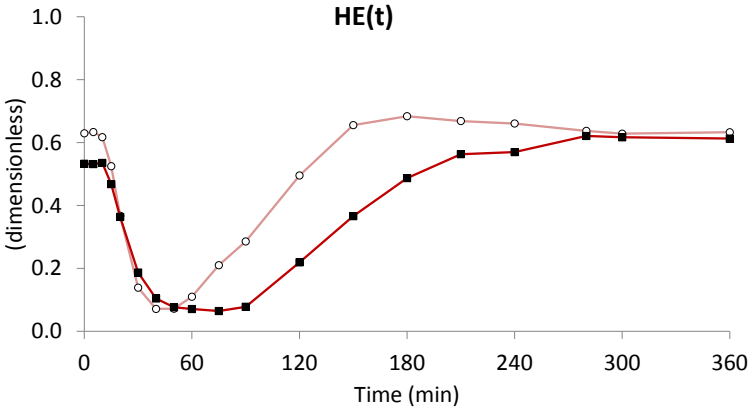

Figure 7.3: Average HE profiles of NGT (◯) and IFG/IGT (■) subjects, in *database 2*, during meal.

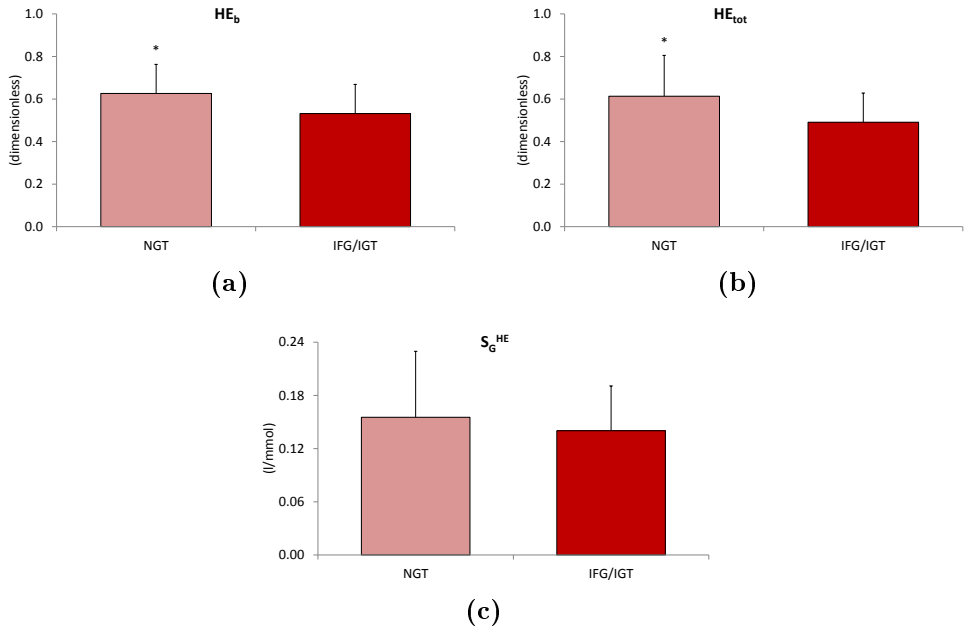

Figure 7.4: Average HE_b (a), HE_{tot} (b), and S_G^{HE} (c) indexes of NGT and IFG/IGT subjects, in *database 2*, during meal. * $p < 0.05$.

this figure, insulin seems not to be well fitted, on average, in t = 20 min, and this is due to approximately 10% of the subjects.
Given that, during the OGTT, the time grid is shorter and under-sampled compared to the MTT (see paragraph 4.3), in this case it was necessary to use a Bayesian approach in order to improve the precision of the parameter estimates, in approximately 20% of the subjects, especially for the parameters V_P and α, included, respectively, in the insulin and C-peptide kinetics; this may in part explain the worsening of model fit in t = 20 min. The mean and SD used in the MAP estimator for these two parameters are, respectively:

$$V_P: \quad mean(V_P) = 0.04, \quad SD(V_P) = 0.2 \cdot mean(V_P) \tag{7.1}$$

$$\alpha: \quad mean(\alpha) = 0.09, \quad SD(\alpha) = 0.5 \cdot mean(\alpha) \tag{7.2}$$

where, for V_P, the mean value was chosen by considering the estimate res-

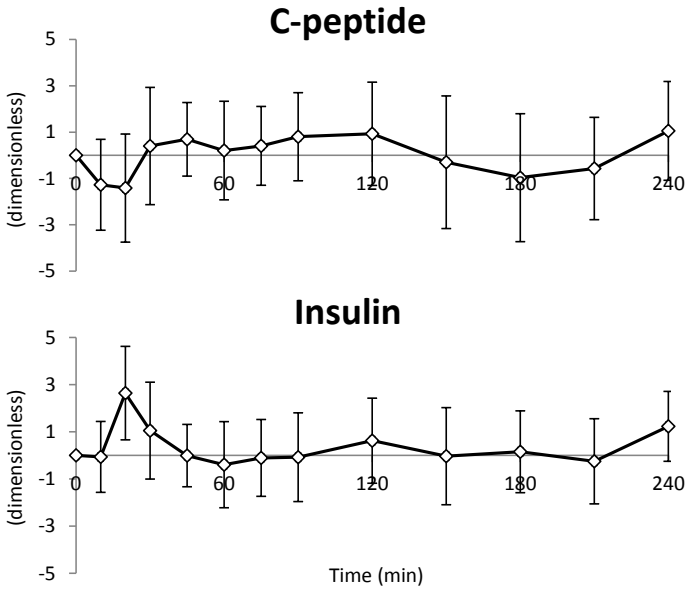

Figure 7.5: Average C-peptide (*top* panel) and insulin (*bottom* panel) weighted residuals, in *database 2*, during OGTT (vertical bars represent ± SD).

ulting from the meal test, and a SD corresponding to 20% of the mean was

shown to be sufficient, while, for α, mean and SD are the ones typically used in the oral C-peptide minimal model, when needed.
The OGTT parameter estimates and CV are shown in Table 7.2, demonstrating the good model performance also in this case.

Unlike what happened during the MTT, in the OGTT the HE indexes did not differ between NGT and IFG/IGT. A possible explanation can be found in the different nutrients that affect the MTT and OGTT insulin secretion and clearance. In particular, it has been shown that amino acids may stimulate insulin secretion [9], and that free fatty acids may directly interfere with insulin clearance [21, 32]. Our results indicate that the effect of other nutrients on HE may be different in healthy and prediabetic subjects.

Table 7.2: Parameter estimates and precision (CV), in *database 2*, during OGTT.

Parameters	**Units**	**Estimates (mean±SD)**	**CV (%)**
$\mathbf{V_P}$	(l/kg)	0.056±0.046	37
$\mathbf{a_G}$	(l/mmol)	0.138±0.098	18
$\mathbf{m_4}$	($\min^{-1}$)	0.468±0.360	30
$\mathbf{m_5}$	($\min^{-1}$)	0.155±0.115	40
$\mathbf{m_6}$	($\min^{-1}$)	0.013±0.009	50
$\mathbf{m_1}$	($\min^{-1}$)	0.917±0.750	32
$\boldsymbol{\alpha}$	($\min^{-1}$)	0.113±0.115	20
$\mathbf{\Phi}_d$	(10^{-9})	568.4±325.5	13
$\mathbf{\Phi}_s$	(10^{-9} $\min^{-1}$)	28.88±12.11	6
$\mathbf{h}$	(mmol/l)	5.264±1.062	4

7.3 Database 3

As highlighted in chapter 4, *database 3* is made up of 14 T2DM and 11 healthy subjects. In the following paragraphs the model performances are shown in both these groups, then focusing on the comparison of HE results.

7.3.1 Healthy subjects

Model VI can quite well predict both C-peptide and insulin data in the healthy subjects composing *database 3* [4], as evident from the average weighted residuals shown in Fig. 7.6 (C-peptide and insulin, *top* and *bottom* panel, respectively). Moreover, the model can precisely estimate the parameters (see Table 7.3).

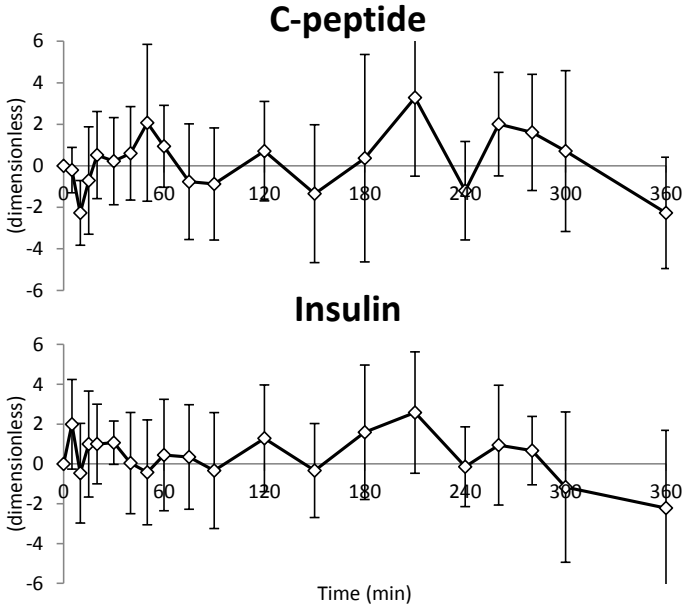

Figure 7.6: Average C-peptide (*top* panel) and insulin (*bottom* panel) weighted residuals of healthy subjects, in *database 3* (vertical bars represent ± SD).

7.3.2 T2DM subjects

Model VI can comprehensively well predict both C-peptide and insulin data also in the T2DM subjects composing *database 3* [4], as shown by the average weighted residuals in Fig. 7.7 (C-peptide and insulin, *top* and *bottom* panel, respectively). However, the average C-peptide and insulin weighted residuals do not always appear to be random.

The parameters are precisely estimated, even if, on average, the CV are a

Table 7.3: Parameter estimates and precision (CV) of healthy subjects, in *database 3*.

Parameters	Units	Estimates (mean±SD)	CV (%)
$\mathbf{V_P}$	(l/kg)	0.028±0.008	16
$\mathbf{a_G}$	(l/mmol)	0.113±0.049	13
$\mathbf{m_4}$	($\min^{-1}$)	0.534±0.285	17
$\mathbf{m_5}$	($\min^{-1}$)	0.257±0.085	27
$\mathbf{m_6}$	($\min^{-1}$)	0.014±0.008	29
$\mathbf{m_1}$	($\min^{-1}$)	1.214±0.596	27
$\boldsymbol{\alpha}$	($\min^{-1}$)	0.188±0.166	26
$\mathbf{\Phi_d}$	(10^{-9})	672.8±252.0	7
$\mathbf{\Phi_s}$	(10^{-9} $\min^{-1}$)	45.48±12.80	2
$\mathbf{h}$	(mmol/l)	4.637±0.432	1

bit higher in this group, compared to healthy subjects, as it usually happens (see Table 7.4).

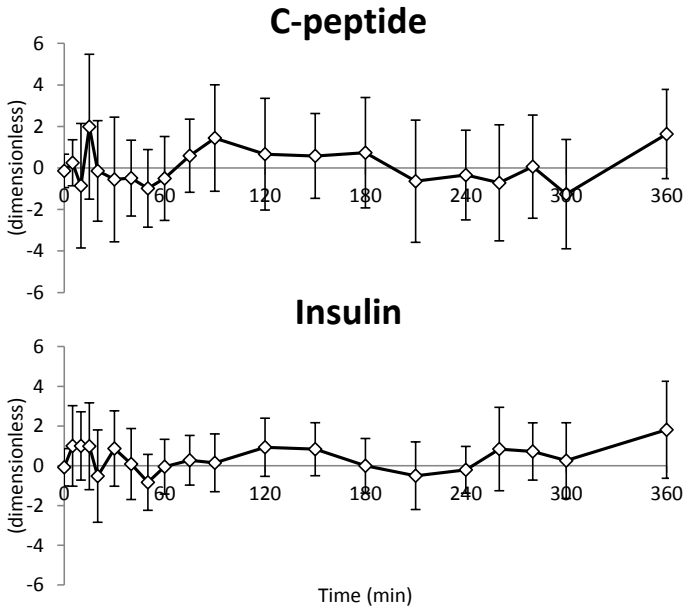

Figure 7.7: Average C-peptide (*top* panel) and insulin (*bottom* panel) weighted residuals of T2DM subjects, in *database 3* (vertical bars represent ± SD).

Table 7.4: Parameter estimates and precision (CV) of T2DM subjects, in *database 3*.

Parameters	Units	Estimates (mean±SD)	CV (%)
$\mathbf{V_P}$	(l/kg)	0.038±0.019	38
$\mathbf{a_G}$	(l/mmol)	0.080±0.047	18
$\mathbf{m_4}$	($\min^{-1}$)	0.705±0.401	38
$\mathbf{m_5}$	($\min^{-1}$)	0.193±0.172	43
$\mathbf{m_6}$	($\min^{-1}$)	0.021±0.010	43
$\mathbf{m_1}$	($\min^{-1}$)	0.635±0.761	28
$\boldsymbol{\alpha}$	($\min^{-1}$)	0.030±0.035	14
$\mathbf{\Phi_d}$	(10^{-9})	311.1±263.9	13
$\mathbf{\Phi_s}$	(10^{-9} $\min^{-1}$)	18.29±9.63	12
$\mathbf{h}$	(mmol/l)	6.489±3.226	17

7.3.3 Healthy vs. T2DM subjects

In the matter of HE in healthy vs. T2DM subjects, the average profiles representing these two groups differ significantly (see Fig. 7.8): the basal level, as well as the whole curve, is lower in T2DM, confirming what was expected, i.e. that HE is reduced when the pathology level increases.
These observations are even more evident when considering the HE indexes, represented in Fig. 7.9, where HE_b, HE_{tot}, and also S_G^{HE} are significantly higher in healthy then T2DM subjects ($HE_b = 0.655\pm0.135$ vs. 0.386 ± 0.149, $p < 0.05$; $HE_{tot} = 0.574\pm0.199$ vs. 0.195 ± 0.130, $p < 0.05$; $S_G^{HE} = 0.113\pm0.049$ vs. 0.080 ± 0.049 l/mmol, $p < 0.05$, respectively).

7.4 Database 4

As mentioned in chapter 4, 14 T2DM subjects were studied after the administration of vildagliptin or placebo, received in random order [16]. The peculiarity of this protocol is the intravenous insulin infusion (0.02 unit/kg of BW) that was administrated over a 5-min period, starting at t=300 min, in order to allow a better estimate of insulin kinetic parameters.

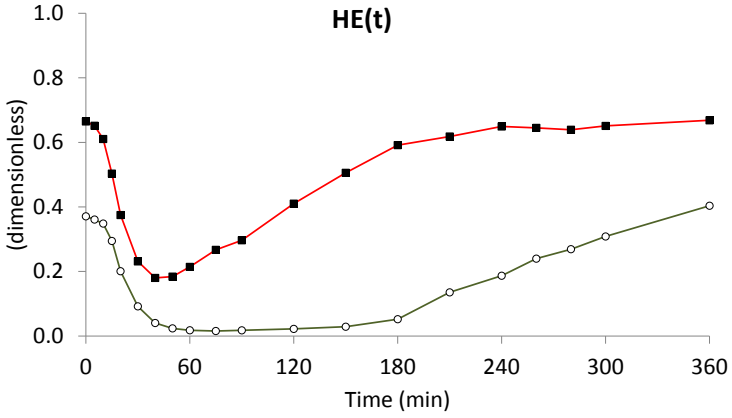

Figure 7.8: Average HE profiles of healthy (■) and T2DM (◯) subjects, in *database 3*.

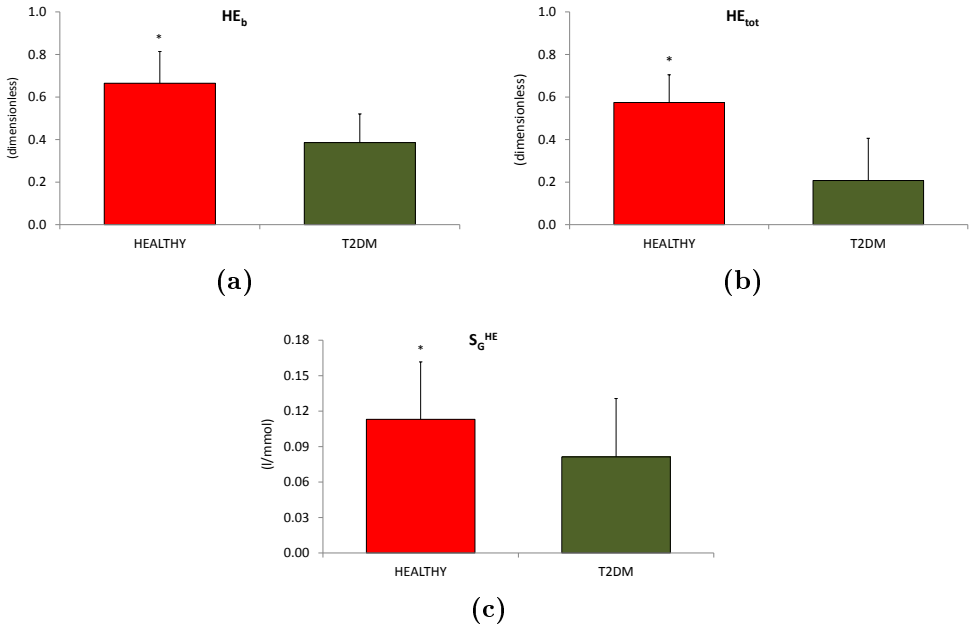

Figure 7.9: Average HE_b (a), HE_{tot} (b), and S_G^{HE} (c) indexes of healthy and T2DM subjects, in *database 3*. * $p < 0.05$.

This allowed performance of two different identifications, and comparison of the results. The first identification includes all the data samples in $0 \div 360$ min, while the second one just employs the data collected before the insulin infusion, i.e. $0 \div 300$ min.

7.4.1 Identification in $[0 \div 360]$ min

Model VI can fit C-peptide and insulin data reasonably well in *database 4* [16], both after placebo and vildagliptin administration (see average weighted residuals in Fig. 7.10-7.11, C-peptide and insulin, *top* and *bottom* panel, respectively). Obviously, the insulin infusion starting in t = 300 min made it difficult to fit the insulin sample drawn at t = 302 min, which is discarded when it falls in a rapid rising edge, in order to improve the whole fit; this fact is responsible for the very low value of insulin weighted residuals at that time point.

The parameters are precisely estimated in both the cases, as shown in Tables

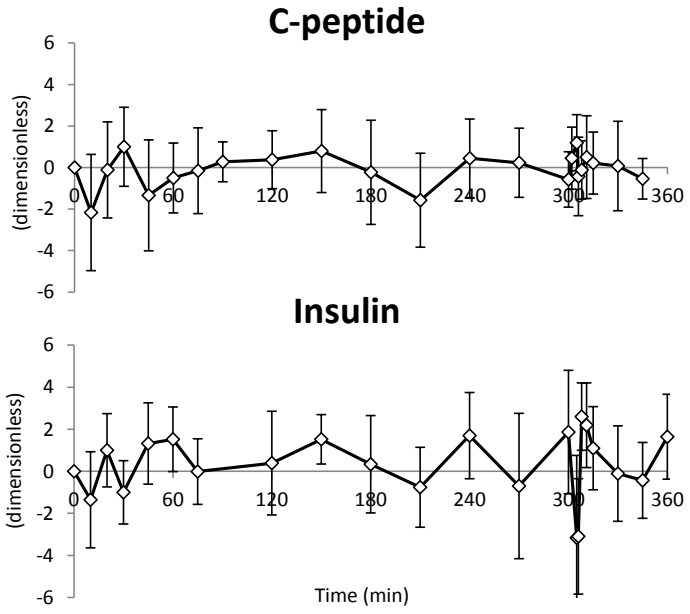

Figure 7.10: Average C-peptide (*top* panel) and insulin (*bottom* panel) weighted residuals, in *database 4* after placebo administration (identification in $0 \div 360$ min; vertical bars represent $\pm$ SD).

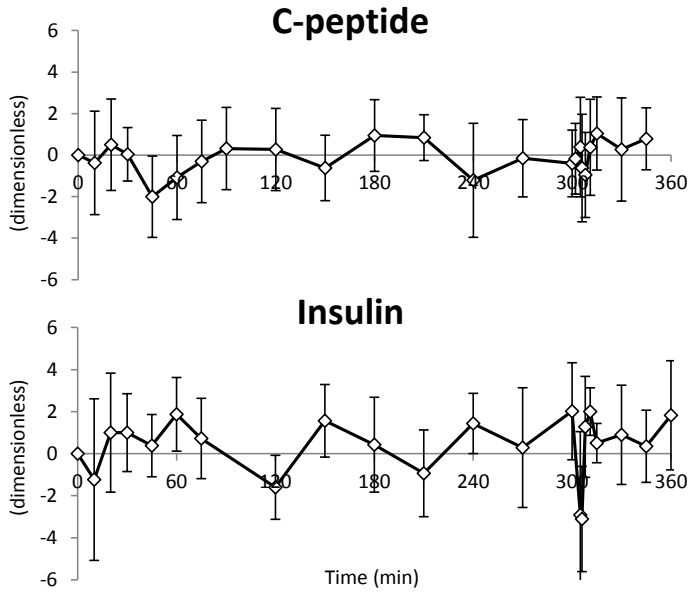

Figure 7.11: Average C-peptide (*top* panel) and insulin (*bottom* panel) weighted residuals, in *database 4* after vildagliptin administration (identification in $0 \div 360$ min; vertical bars represent ± SD).

7.5-7.6. Thanks to the peculiarity of this protocol, which includes the insulin infusion, it was also possible to well estimate the parameter m_2, that was usually fixed to a standard value ($m_2 = 0.268$ min^{-1}, in *database 1, 2, 3*).

The average HE profiles are very similar after placebo and vildagliptin administration (Fig. 7.12). This observation is strengthened by the statistical tests performed on the HE indexes (see Fig. 7.13): no significant difference is found in presence of placebo or vildagliptin ($HE_b = 0.433 \pm 0.162$ vs. 0.467 ± 0.196, $p > 0.05$; $HE_{tot} = 0.370 \pm 0.195$ vs. 0.394 ± 0.234, $p > 0.05$; $S_G^{HE} = 0.076 \pm 0.48$ vs. 0.094 ± 0.57 l/mmol, $p > 0.05$, respectively), confirming the results found in the previous work [16], using the *Model of Data*.

7.4.2 Identification in $[0 \div 300]$ min

Just identifying the first 300 minutes of the protocol, i.e. excluding the insulin infusion, *Model VI* can adequately predict the data (see Fig. 7.14-7.15) and the parameters are estimated with a good precision (see Tables

Table 7.5: Parameter estimates and precision (CV), in *database 4* after placebo administration (identification in $0 \div 360$ min).

Parameters	Units	Estimates (mean±SD)	CV (%)
$\mathbf{V_P}$	(l/kg)	0.061±0.019	8
$\mathbf{a_G}$	(l/mmol)	0.076±0.048	18
$\mathbf{m_4}$	($\min^{-1}$)	0.474±0.245	14
$\mathbf{m_5}$	($\min^{-1}$)	0.345±0.095	56
$\mathbf{m_6}$	($\min^{-1}$)	0.084±0.073	47
$\mathbf{m_1}$	($\min^{-1}$)	0.652±0.503	56
$\mathbf{m_2}$	($\min^{-1}$)	0.356±0.496	36
$\boldsymbol{\alpha}$	($\min^{-1}$)	0.051±0.035	23
$\mathbf{\Phi}_d$	(10^{-9})	205.2±198.1	58
$\mathbf{\Phi}_s$	(10^{-9} $\min^{-1}$)	17.89±13.80	7
$\mathbf{h}$	(mmol/l)	5.456±1.622	9

Table 7.6: Parameter estimates and precision (CV), in *database 4* after vildagliptin administration (identification in $0 \div 360$ min).

Parameters	Units	Estimates (mean±SD)	CV (%)
$\mathbf{V_P}$	(l/kg)	0.062±0.034	7
$\mathbf{a_G}$	(l/mmol)	0.094±0.057	17
$\mathbf{m_4}$	($\min^{-1}$)	0.410±0.153	13
$\mathbf{m_5}$	($\min^{-1}$)	0.381±0.058	24
$\mathbf{m_6}$	($\min^{-1}$)	0.071±0.061	30
$\mathbf{m_1}$	($\min^{-1}$)	0.594±0.438	54
$\mathbf{m_2}$	($\min^{-1}$)	0.394±0.438	43
$\boldsymbol{\alpha}$	($\min^{-1}$)	0.050±0.031	16
$\mathbf{\Phi}_d$	(10^{-9})	226.9±164.0	16
$\mathbf{\Phi}_s$	(10^{-9} $\min^{-1}$)	17.58±9.248	7
$\mathbf{h}$	(mmol/l)	5.946±2.561	6

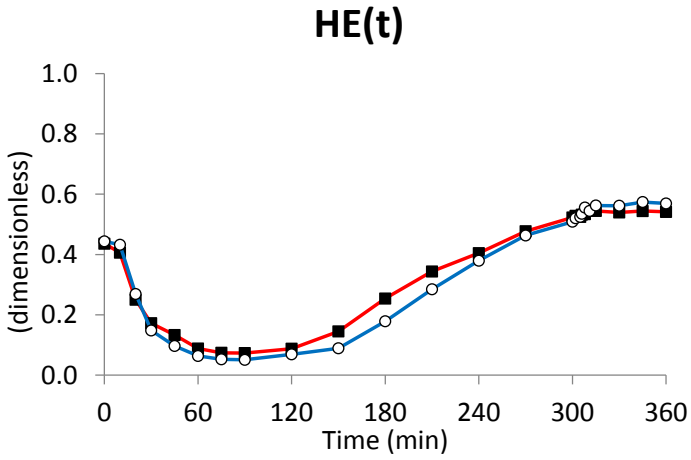

Figure 7.12: Average HE profiles in *database 4* after placebo (■) and vildagliptin (◯) administration (identification in $0 \div 360$ min).

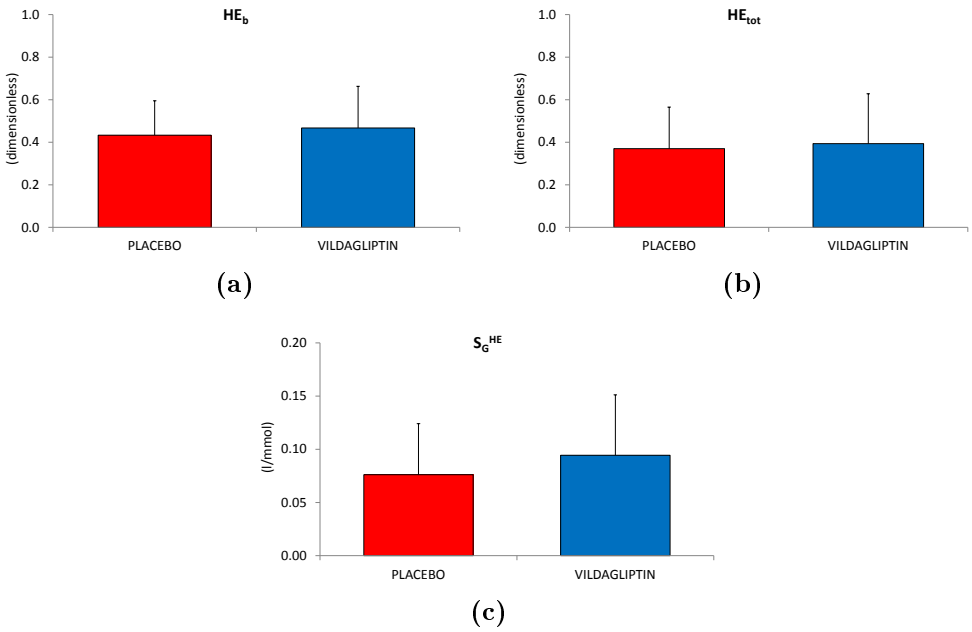

Figure 7.13: Average HE_b (a), HE_{tot} (b), and S_G^{HE} (c) indexes in *database 4* after placebo and vildagliptin administration (identification in $0 \div 360$ min).

7.7-7.8), in the presence of placebo and vildagliptin. As expected, the CV are higher on average if compared to the ones shown in Tables 7.5-7.6, because of the absence of insulin infusion.

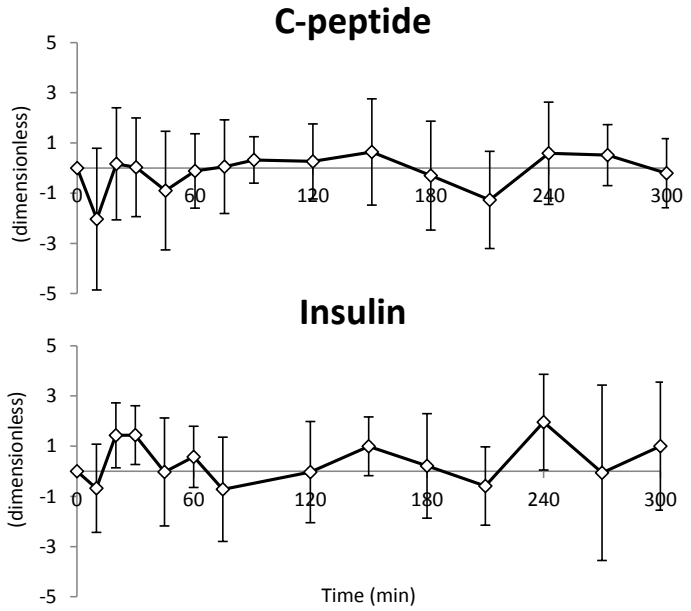

Figure 7.14: Average C-peptide (*top* panel) and insulin (*bottom* panel) weighted residuals, in *database 4* after placebo administration (identification in $0 \div 300$ min; vertical bars represent $\pm$ SD).

Table 7.7: Parameter estimates and precision (CV), in *database 4* after placebo administration (identification in $0 \div 300$ min).

Parameters	**Units**	**Estimates (mean±SD)**	**CV (%)**
$\mathbf{V_P}$	(l/kg)	0.062±0.022	34
$\mathbf{a_G}$	(l/mmol)	0.112±0.069	24
$\mathbf{m_4}$	($\min^{-1}$)	0.446±0.233	42
$\mathbf{m_5}$	($\min^{-1}$)	0.262±0.163	51
$\mathbf{m_6}$	($\min^{-1}$)	0.020±0.015	63
$\mathbf{m_1}$	($\min^{-1}$)	1.059±0.849	42
$\boldsymbol{\alpha}$	($\min^{-1}$)	0.043±0.021	25
$\boldsymbol{\Phi_d}$	(10^{-9})	237.2±125.5	30
$\boldsymbol{\Phi_s}$	(10^{-9} $\min^{-1}$)	17.18±10.03	12
$\mathbf{h}$	(mmol/l)	6.311±2.413	13

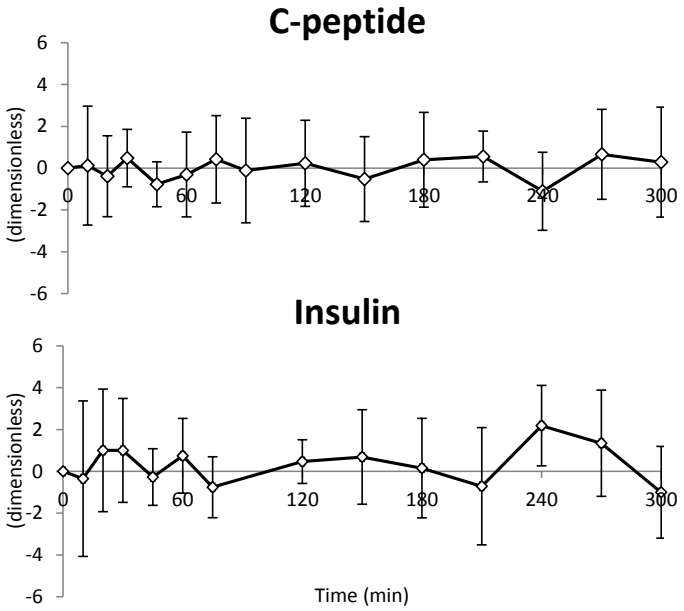

Figure 7.15: Average C-peptide (*top* panel) and insulin (*bottom* panel) weighted residuals, in *database 4* after vildagliptin administration (identification in $0 \div 300$ min; vertical bars represent $\pm$ SD).

Table 7.8: Parameter estimates and precision (CV), in *database 4* after vildagliptin administration (identification in $0 \div 300$ min).

Parameters	**Units**	**Estimates (mean±SD)**	**CV (%)**
$\mathbf{V_P}$	(l/kg)	0.046±0.021	13
$\mathbf{a_G}$	(l/mmol)	0.105±0.062	24
$\mathbf{m_4}$	($\min^{-1}$)	0.473±0.247	25
$\mathbf{m_5}$	($\min^{-1}$)	0.236±0.162	33
$\mathbf{m_6}$	($\min^{-1}$)	0.011±0.004	73
$\mathbf{m_1}$	($\min^{-1}$)	0.973±0.786	64
$\boldsymbol{\alpha}$	($\min^{-1}$)	0.038±0.015	15
$\mathbf{\Phi_d}$	(10^{-9})	301.0±119.7	23
$\mathbf{\Phi_s}$	(10^{-9} $\min^{-1}$)	22.59±7.970	10
$\mathbf{h}$	(mmol/l)	6.735±2.979	7

As regards HE, the average profiles, in the presence of placebo and vildagliptin, are reported in Fig. 7.16. In this case, the average vildagliptin profile seems a bit higher than observed with placebo, whereas in "0÷360 min" the difference was quite imperceptible. However, the statistical tests performed on HE indexes (see Fig. 7.17) show no significant difference in placebo vs. vildagliptin (HE_b = 0.471±0.187 vs. 0.566±0.123, p > 0.05; HE_{tot} = 0.362±0.249 vs. 0.418±0.228, p > 0.05; S_G^{HE} = 0.112±0.069 vs. 0.105±0.062 l/mmol, p > 0.05, respectively).

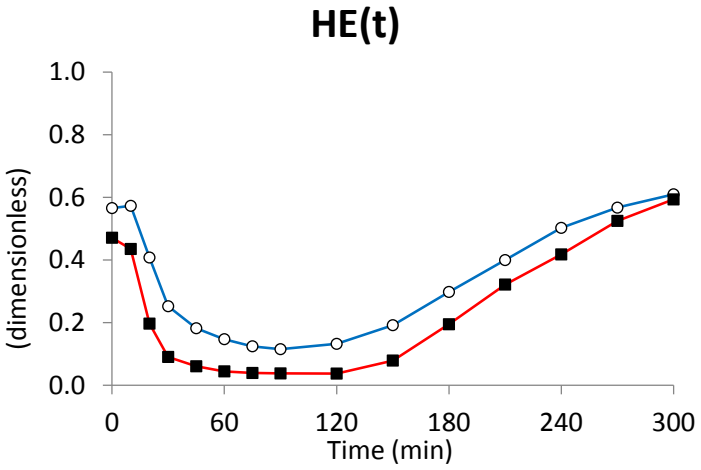

Figure 7.16: Average HE profiles in *database 4*, after placebo (■) and vildagliptin (◯) administration (identification in 0 ÷ 300 min).

7.4.3 Comparison

The HE indexes obtained in both the identifications performed in *database 4* ("0 ÷ 360 min" and "0 ÷ 300 min") were compared in order to assess how much the optimal estimate of insulin kinetics may change the results obtained in sub-obtimal conditions (see average values in Table 7.9). It is of note that, for this kind of analysis, all the subjects were considered together, no matter of placebo or vildagliptin administration, for the purpose of increasing the power of the test.

In Fig. 7.18 the correlation analysis performed on HE_b, HE_{tot}, S_G^{HE} and

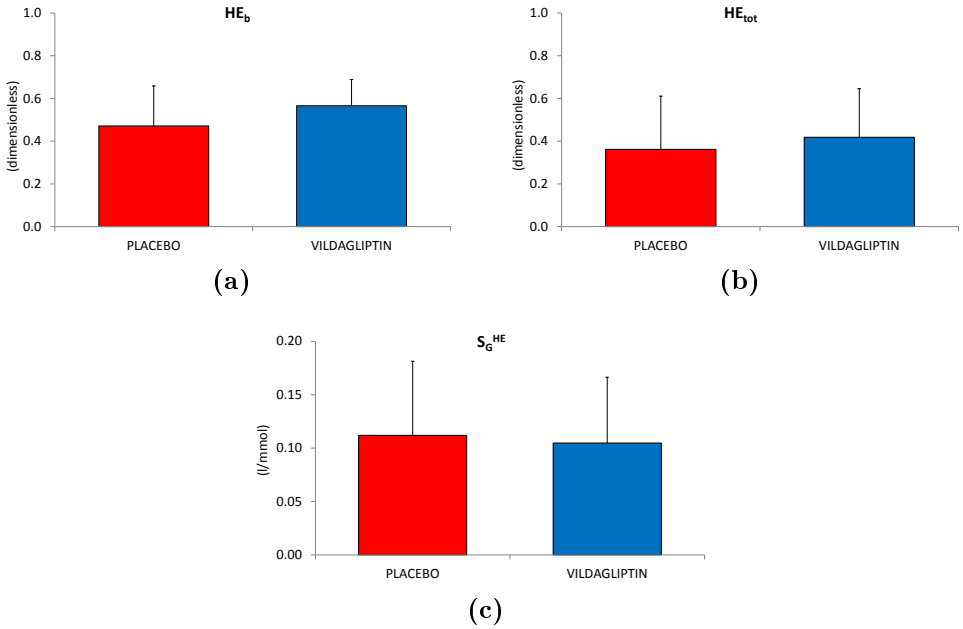

Figure 7.17: Average HE_b (a), HE_{tot} (b), and S_G^{HE} (c) indexes in *database 4* after placebo and vildagliptin administration (identification in $0 \div 300$ min).

insulin clearance ($CL_I = m_4 \cdot V_P$) are shown, and, clearly, all these indexes provide a significant correlation between the two cases (R = 0.57, p < 0.005 for HE_b; R = 0.70, p < 0.005, for HE_{tot}; R = 0.84, p < 0.005, for S_G^{HE}; R = 0.87, p < 0.005, for CL_I). This result confirms that *Model VI* does not need the use of an exogenous insulin infusion in order to obtain reliable HE oral indexes.

Table 7.9: HE indexes in "$0 \div 300$ min" vs. "$0 \div 360$ min" identification.

Index	Units	"$0 \div 300$ min" estimates (mean±SD)	"$0 \div 360$ min" estimates (mean±SD)
$\mathbf{HE_b}$	(dimensionless)	0.519±0.163	0.450±0.176
$\mathbf{HE_{tot}}$	(dimensionless)	0.390±0.235	0.382±0.211
$\mathbf{S_G^{HE}}$	(l/mmol)	0.108±0.064	0.085±0.062
$\mathbf{CL_I}$	(l/kg/min)	0.023±0.014	0.025±0.011

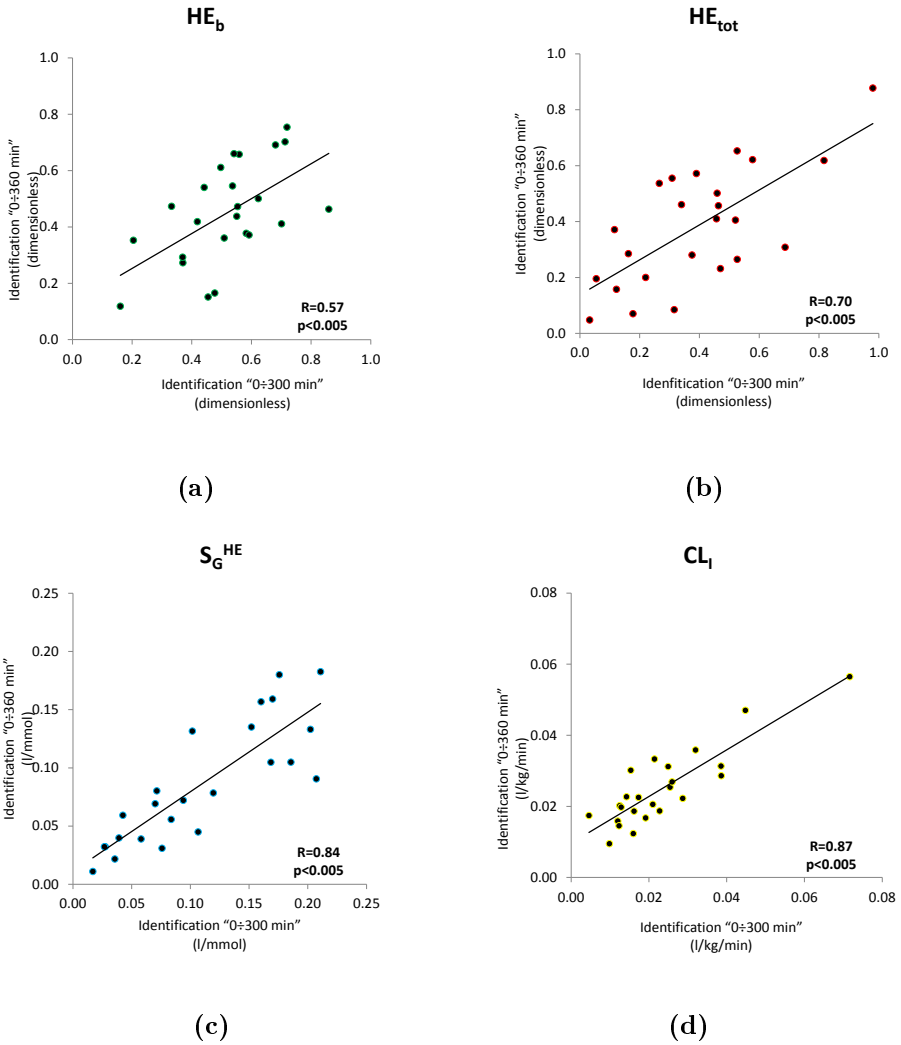

Figure 7.18: HE_b (a), HE_{tot} (b), S_G^{HE} (C) and CL_I (d) indexes: correlation between the identification in "$0 \div 360$ min" and "$0 \div 300$ min".

8 Conclusions

Glucose metabolism is regulated by a complex control system, which, in healthy subjects, maintains plasma glucose concentration within a narrow range, in order to avoid hypoglycemia or hyperglycemia.
The liver plays an important role in glucose regulation, since, besides producing glucose, it is also responsible for regulating insulin levels, by extracting a significant portion of the insulin appearing in the portal vein (approximately 50%) [12], during first pass transit. Therefore, the quantification of HE, in basal as well as in dynamic conditions, is an essential step to understand the overall glucose metabolism.
Since direct measurement of HE in humans is very invasive, requiring catheter insertion in the portal and hepatic veins, the only effective method for assessing HE is the use of mathematical models, that utilize the measurements of plasma insulin, glucose and C-peptide concentrations. Indeed, at the base of these models, there is the known concept that C-peptide and insulin are equimolarly secreted, but only insulin is extracted by the liver; this fact allows conception of models which describe insulin, and thus C-peptide, secretion, and kinetics, including HE.

Toffolo et al. [50] assessed HE during an IM-IVGTT, using a model of C-peptide secretion and kinetics, previously developed in [10] and [24], respectively, where C-peptide parameters were fixed according to [55], and

single-compartment insulin kinetics, in which the parameters could be estimated from an insulin infusion. In order to extend this approach to a meal test, Campioni et al. [11] developed a *Model of Data*. Since both C-peptide and insulin kinetic parameters were there fixed, according to [55] and [11], respectively, HE was described as a piecewise linear function with seven breakpoints; the values of HE were parameters to be estimated by fitting the model to insulin data. This approach certainly allows the HE parameters to obtain a good fit of meal insulin data. On the other hand, the HE formulation does not have a physiological or mechanistic meaning which makes the model vulnerable to noise, since it can follow rapid peripheral insulin fluctuations.

In order to improve HE assessment, the aim of this thesis is to propose a model which contains a broader description of insulin kinetics, and a more physiological expression of HE. Therefore, the single- [11], two- [17, 26], and three- [17, 26] compartment insulin kinetic models were tested, coupled with the new HE descriptions, depending on plasma glucose and insulin concentrations, alone and in combination. In so doing, seven new models were developed, and compared to the *Model of Data*, proposed by Campioni et al. According to the results, the best performing model was *Model VI*, which describes insulin kinetics with three compartments, and assumes that HE depends on glucose concentration.
The new model has a concrete physiological meaning: it describes insulin kinetics through liver, plasma and extravascular spaces, according to previous studies conducted first in dogs and then in humans [25, 26, 47]. Moreover, HE is a function of plasma glucose, supporting the nutrient intake influence on HE, and, especially, the HE reduction due to hyperglycemia [20, 31, 42].

The new model was first assessed in *database 1*, the same one adopted by Campioni et al., made up of 204 healthy subjects, that underwent a FS-MTT. Besides showing good performance in terms of data prediction and parameter estimates, it offers many advantages, with respect to the model available in the literature. First of all, it can well estimate all the insulin kinetic parameters, differently from the *Model of Data*, in which they

were fixed to standard population values. Secondly, it describes HE using a single parameter, thus overcoming one of the main limitations of the model developed by Campioni et al., where the HE profile was allowed to rapidly change due to peripheral insulin fluctuations, making the model vulnerable to noise. Finally, the new HE formulation allows derivation of a new index, accounting for HE sensitivity to glucose, i.e. S_G^{HE}; this index was found to be lower in elderly vs. young ($p < 0.05$) and this agrees with the knowledge that glucose control system is impaired in elderly people.
It is of note that this model was originally proposed in a particular frequently sampled meal time grid (FS-MTT) [6], that is not so easily reproducible in a usual experimental setting, because of high costs; however, the model has been shown to perform well even with standard sampling (SS-MTT) [10], providing precise parameter estimates, and well correlated HE indexes ($p < 0.005$) between FS- and SS-MTT.

Once the model was assessed in healthy conditions, we used it in all the spectrum of glucose tolerance (healthy, prediabetic and T2DM subjects), and also during a different oral challenge, i.e. the OGTT.
The model employment in *database 2*, made up of prediabetic subjects with different levels of glucose intolerance, during the MTT, was successful, since the model could adequately fit the data and estimate the parameters; moreover, HE indexes (HE_b and HE_{tot}) are lower in IFG/IGT than NGT subjects ($p<0.05$), thus confirming the knowledge that HE is impaired in conditions of glucose intolerance.
Having also the OGTT data of the same database, it was interesting to realize that the model performances were good, too, underlying that the effects of nutrient intake on HE may be different among healthy and prediabetics.
Then, the model was used in *database 3*, made up of T2DM and healthy people, who underwent a MTT; the data were well fitted in both the groups, and the parameters were precisely estimated, even if the T2DM CV were a little bit higher. In this case, all the HE indexes (HE_b, HE_{tot} and S_G^{HE}) were significantly lower ($p<0.05$) in T2DM subjects, supporting the awareness of lower HE in pathological conditions.
Finally, the model was used in *database 4*, composed of T2DM subjects,

treated with placebo and vildagliptin, who underwent a particular MTT, characterized by a 5-min square wave insulin infusion, which should allow a better estimation of insulin kinetics. In this case, two different identifications were performed: the first one ("0÷360 min"), by considering the entire protocol samples, and the second one ("0÷300 min"), by neglecting the insulin infusion. In both the identifications, no HE difference was revealed among the placebo and vildagliptin treatments, thus confirming what was previously found [16]. Interestingly, all the HE indexes, and the insulin clearance rate, showed a significant correlation between the "0÷300" and "0÷360" min identification; this result is very important for the proposed model, since it means there is no need to add an insulin infusion to the experiment in order to estimate reliable HE indexes.

In conclusion, the present study demonstrates that the HE model proposed by Campioni et al., which currently predicts data well, can be improved by adopting a three-compartment model for the description of insulin kinetics, and by substituting the piecewise linear function with a simple linear expression which links HE to plasma glucose concentration.
The new model can well describe insulin and C-peptide data during both MTT and OGTT, in all the spectrum of glucose tolerance, with the peculiarity of providing a new index of HE sensitivity to glucose, which has potential to help in distinguishing different levels of pathology.
Future developments would be the introduction of this new model in the meal simulation model of the glucose-insulin system [17], replacing the pre-existent two-compartment insulin kinetics, and the linear relationship that links HE to insulin secretion, which suffers from some limitations when predicting HE in a given individual. Further studies will be required to assess the validity of this model during different tests, e.g. IM-IVGTT.

Bibliography

[1] **Akiyama H., Yokono K., Shii K., Ogawa W., Taniguchi H., Baba S., Kasuga M.**, Natural regulatory mechanisms of insulin degradation by insulin degrading enzyme, *Biochem Biophys Res Commun* 170: 1325-1330, 1990.

[2] **Aronoff S.L., Berkowitz K., Shreiner B., Want L.**, Glucose metabolism and regulation: beyond insulin and glucagon, *Diabetes Spectrum* 17(3): 183-190, 2004.

[3] **Backer J.M., Kahn C.R., White M.F.**, The dissociation and degradation of internalized insulin occur in the endosomes of rat hepatoma cells, *J Biol Chem* 265: 14828-14835, 1990.

[4] **Basu A., Dalla Man C., Basu R., Toffolo G., Cobelli C., Rizza R.A.**, Effects of type 2 diabetes on insulin secretion, insulin action, glucose effectiveness, and postprandial glucose metabolism, *Diabetes Care* 32(5): 866-872, 2009.

[5] **Basu R., Di Camillo B., Toffolo G., Basu A., Shah P., Vella A., Rizza R.A., Cobelli C.**, Use of a novel triple-tracer approach to assess postprandial glucose metabolism, *Am J Physiol Endocrinol Metab* 284: E55-E69, 2003.

[6] **Basu R., Dalla Man C., Campioni M., Basu A., Klee G., Toffolo G., Cobelli C., Rizza R.A.**, Effects of age and sex on postprandial glucose metabolism: differences in glucose turnover, insulin secretion, insulin action, and hepatic insulin extraction, *Diabetes* 55: 2001-2014, 2006.

[7] **Bellu G., Saccomani M.P., Audoly S., D'Angiò L.**, DAISY: A new software tool to test global identifiability of biological and physiological systems, *Comput Methods Programs Biomed* 88(1): 52-61, 2007.

[8] **Bock G., Dalla Man C., Campioni M., Chittilapilly E., Basu R., Toffolo G., Cobelli C., Rizza R.A.**, Mechanisms of fasting and postprandial hyperglycemia in people with impaired fasting glucose and/or impaired glucose tolerance, *Diabetes* 55: 3536-3529, 2006.

[9] **Bock G., Dalla Man C., Campioni M., Chittilapilly E., Basu R., Toffolo G., Cobelli C., Rizza R.A.**, Effects of nonglucose nutrients on insulin secretion and action in people with pre-diabetes, *Diabetes* 56(4): 1113-1119, 2007.

[10] **Breda E., Cavaghan M.K., Toffolo G., Polonsky K.S., Cobelli C.**, Oral glucose tolerance test minimal model indexes of beta-cell function and insulin sensitivity, *Diabetes* 50: 150-158, 2001.

[11] **Campioni M., Toffolo G., Basu R., Rizza R.A., Cobelli C.**, Minimal model assessment of hepatic insulin extraction during an oral test from standard insulin kinetics parameters, *Am J Physiol Endocrinol Metab* 297: E941-E948, 2009.

[12] **Caumo A., Florea I., Luzi L.**, Effect of variable hepatic insulin clearance on the postprandial insulin profile: insights from a model simulation study, *Acta Diabetol* 44: 23-29, 2007.

[13] **Cobelli C., Carson E.**, Introduction to modeling in physiology and medicine, *Academic Press, San Diego*, 2008.

[14] **Cobelli C., Pacini G.**, Insulin secretion and hepatic extraction in humans by minimal modeling of C-peptide and insulin data, *Diabetes* 37: 223-231, 1988.

[15] **Cobelli C., Toffolo G.M., Dalla Man C., Campioni M., Denti P., Caumo A., Butler P.C., Rizza R.A.**, Assessment of β-cell function in humans, simultaneously with insulin sensitivity and hepatic extraction, from intravenous and oral glucose test, *Am J Physiol Endocrinol Metab* 293: E1-E15, 2007.

[16] **Dalla Man C., Bock G., Giesler P.D., Serra D.B., Saylan M.L., Foley J.E., Camilleri M., Toffolo G., Cobelli C., Rizza R.A., Vella A.**, Dipeptidyl peptidase-4 inhibition by vildagliptin and the effect on insulin secretion and action in response to meal ingestion in type 2 diabetes, *Diabetes Care* 32(1): 14-18, 2009.

[17] **Dalla Man C., Rizza R.A., Cobelli C.**, Meal simulation model of the glucose-insulin system., *IEEE Trans on Biomed Eng* 54(10): 1740-1749, 2007.

[18] www.diabetes.org

[19] **Dinneen S.F., Maldonado D. 3rd, Leibson C.L., Klee G.G., Li H., Melton L.J. 3rd, Rizza R.A.**, Effects of changing diagnostic criteria on the risk of developing diabetes, *Diabetes Care* 21: 1408-1413, 1998.

[20] **Duckworth C.W.**, Insulin degradation: mechanisms, products and significance, *Endoc Rev* 2: 210-233, 1988.

[21] **Duckworth W.C., Bennet G.B., Hamel F.G.**, Insulin degradation: progress and potential, *Endocr Rev* 19(5): 608-624, 1998.

[22] **Duckworth W.C., Runyan K., Wright R.K., Halban P.A., Solomon S.S.**, Insulin degradation by hepatocytes in primary colture, *Endocrinology* 108: 1142-1147, 1981.

[23] www.easd.org

[24] **Eaton R.P., Allen R.C., Schade D.S., Erickson K.M., Standefer J.**, Prehepatic insulin production in man: kinetic analysis using peripheral connecting peptide behaviour, *J Clin Endocrinol Metab* 51: 520-528, 1980.

[25] **Ellmerer M., Hamilton-Wessler M., Kim S.P., Dea M.K., Kirkman E., Perianayagam A., Markussen J., Bergman R.N.**, Mechanism of Action in Dogs of Slow-Acting Insulin Analog O346, *J Endocrinol Metab* 88(5): 2256-2262, 2003.

[26] **Ferrannini E., Cobelli C.**, The kinetics of insulin in man. II. Role of the liver, *Diabetes Metab Rev* 3: 365-397, 1987.

[27] **Greenway C.V., Stark R.D.**, Hepatic vascular bed, *Physiol Rev* 51(1): 23-65, 1971.

[28] **Hamel F.G., Mahoney M.J., Duckworth W.C.**, Degradation of intraendosomal insulin by insulin degrading enzyme without acidification, *Diabetes* 40: 436-433, 1991.

[29] **Hamel F.G., Peavy D.E., Ryan M.P., Duckworth WC.**, High performance liquid chromatographic analysis of insulin degradation products from isolated hepatocytes: effects of hinibitors suggest intracellular and extracellular pathways, *Diabetes* 36: 702-708, 1987.

[30] **Harada S., Smith R.M., Smith J.A., Shah N., Jarett L.**, Demonstration of specific insulin binding to cytosolic proteins in H35 hepatoma cells, rat liver, and skeletal muscle, *Biochem J* 306: 21-28, 1995.

[31] **Hennes M.M., Dua A., Kissebah A.H.**, Effects of free fatty acids and glucose on spalachnic insulin dynamics, *Diabetes* 46: 57-62, 1997.

[32] **Hennes M.M., Shrago E., Kissebah A.H.**, Mechanism of free fatty acid effects on hepatocyte insulin receptor binding and processing, *Obes Res* 1(1): 18-28, 1993.

[33] www.idf.org

[34] **Jensen M.D., Kanaley J.A., Reed J.E., Sheedy P.F.**, Measurement of abdominal and visceral fat with computed tomography and dual-energy x-ray absorptiometry, *Am J Clin Nutr* 61: 274-278, 1995.

[35] **Jochen A., Hays J., Lee M.**, Kinetics of insulin internalization and processing in adipocytes: effects of insulin concentration, *J Cell Physiol* 141: 527-534, 1989.

[36] **Kuo W.L., Gehm B.D., Rosner M.R.**, Regulation of insulin degradation: expression of an evolutionary conserved insulin-degrading enzyme increases degradation via an intracellular pathway, *Mol Endocrinol* 5: 1467-1476, 1991.

[37] **LeRoith D., Taylor S.I., Olefsky J.M.**, Diabetes mellitus: a fundamental and clinical text, *3rd edition, Lippincott Williams & Wilkins*, 2004.

[38] **Levy J., Olefsky J.M.**, The effects of insulin concentration on retroendocytosis in isolated rat adipocytes, *Endocrinology* 120: 450-456, 1987.

[39] **Meier J.J., Veldhuis J.D., Butler P.C.**, Pulsatile insulin secretion dictates systemic insulin delivery by regulating hepatic insulin extraction in humans, *Diabetes* 54(6): 1649-1656, 2005.

[40] **Meigs J.B., Muller D.C., Nathan D.M., Blake D.R., Andres R.**, The natural history of progression from normal glucose tolerance to type 2 diabetes in the Baltimore Longitudinal Study of Aging, *Diabetes* 52: 1475-1484, 2003.

[41] **Pagano C., Rizzato M., Lombardi A.M., Fabris R., Favaro A., Federspil G., Vettor R.**, Effect of lactate on hepatic insulin clearance in perfused rat liver, *Am J Physiol* 270: R682-R687, 1996.

[42] **Pivovarova O., Gogebakan O., Pfeiffer A.F.H., Rudovich N.**, Glucose inhibits the insulin-induced activation of the insulin-degrading enzyme in HepG2 cells, *Diabetologia* 52: 1656-1664, 2009.

[43] **Seabright P.J., Smith G.D.**, The characterization of endosomal insulin degradation intermediates and their sequence of production, *Biochem J* 320: 947-956, 1996.

[44] **Sherwin R.S., Kramer K.J., Tobin J.D., Insel P.A., Liljenquist J.E., Berman M., Andres R.**, A model of the kinetics of insulin in man, *J Clin Invest* 52: 1481-1492, 1974.

[45] **Smith R.M., Jarret L.**, Biology of disease. Receptor-mediated endocytosis and intracellular processing of insulin: ultrastructural and biochemical evidence for cell-specific heterogeneity and distinction from nonhormonal ligands, *In Rubin E., Damjanov I. (eds) Pathology reviews. Humana Press Inc., Clifton, NJ* 37-53, 1989.

[46] **Sonne O.**, Receptor-mediated endocytosis and degradation of insulin, *Physiol Rev* 68(4): 1129-1195, 1988.

[47] **Steil G.M., Ader M., Moore D.M., Rebrin K., Bergman R.N.**, Transendothelial insulin transport is not saturable in vivo, *J Clin Invest* 97(6): 1947-1503, 1996.

[48] **Surmacz C.A., Wert J.J., Ward W.F., Mortimore G.E.**, Uptake and intracellular fate of [^{14}C]sucrose-insulin in perfused rat livers, *Am J Physiol* 255: C70-C75, 1988.

[49] **Svederg J., Bjorntorp P., Smith U., Lonnroth P.**, Free fatty acids inhibition of insulin binding, degradation, and action in isolated rat hepatocytes, *Diabetes* 39: 570-574, 1996.

[50] **Toffolo G., Campioni M., Basu R., Rizza R.A., Cobelli C.**, A minimal model of insulin secretion and kinetics to assess hepatic insulin extraction, *Am J Physiol Endocrinol Metab* 290: E169-E176, 2006.

[51] **Toffolo G., Cefalu W., Cobelli C.**, Beta-cell function during insulin modified IVGTT successfully assessed by the C-peptide minimal model, *Metabolism* 48: 1162-1166, 1999.

[52] **Toffolo G., De Grandi F., Cobelli C.**, Estimation of beta-cell sensitivity from IVGTT C-peptide data. Knowledge of the kinetics avoids errors in modeling the secretion, *Diabetes* 44: 845-854, 1995.

[53] **Tura A., Ludvik B., Nolan J.J., Pacini G., Thomaseth K.**, Insulin and C-peptide secretion and kinetics in humans: direct and model-based measurements during OGTT, *Am J Physiol Endocrinol Metab* 281: E966-E974, 2001.

[54] **Tirosh A., Shai I., Tekes-Manova D., Israeli E., Pereg D., Shochat T., Kochba I., Rudich A., the Israeli Diabetes Research Group**, Normal fasting plasma glucose levels and type 2 diabetes in young men, *N Engl J Med* 353: 1454-1462, 2005.

[55] **Van Cauter E., Mestrez F., Sturie J., Polonsky K.S.**, Estimation of insulin secretion rates from C-peptide levels. Comparison of individual and standard kinetic parameters for C-peptide clearance, *Diabetes* 41: 368-377, 1992.

[56] **Volund A., Polonsky K.S., Bergman R.N.**, Calculated pattern of intraportal insulin appearance without independent assessment of Cpeptide kinetics, *Diabetes* 36: 1195-1202, 1987.

[57] **Wiesenthal S.R., Sandhu H., McCall R.H., Tchipashvili V., Yoshii H., Polonsky K.S., Shi Z.Q., Lewis G.F., Mari A., Giacca A.**, Free fatty acids impair hepatic insulin extraction in vivo, Erratum appears in *Diabetes* 48(4): 766-774, 1999.

[58] **Yonezawa K., Yokono K., Shii K., Hari J., Yaso S., Amano K., Sakamoto T., Kawase Y., Akiyama H., Nagata M., Baba S.**, Insulin-degrading enzyme is capable of degrading receptor-bound insulin , *Biochem Biophys Res Commun* 150: 605-614, 1988.

Acknowledgments

I want to thank Prof. Chiara Dalla Man and Prof. Claudio Cobelli, that both supervised my research work with their constructive suggestions through all these years, and taught me the importance of being independent and hard-working.
I would also like to thank Dr. Adrian Vella, my "abroad advisor", for allowing me to spend a period at Mayo Clinic, working with his extraordinary team; the months I spent collaborating with him in Rochester represent an important research and personal experience, that I will pleasantly remember forever. I need to thank Dr. Adrian Vella also for his constant "distance support", since he has always helped me, even when I came back to Padova.
Thanks to all the friends I met in the bioengineering Ph.D. group, for the funny time we spent together, and for the help they have always given me, especially Chiara, Francesca, Michela, Fabio, Mattia, Anna, Federica, Emanuele and Michele.
Thanks to Giacomo, for being my first supporter, and for always reminding me of my capabilities and qualities.
Grazie a mia mamma, per tutte le volte che mi ha supportata e appoggiata nelle le mie scelte, credendo sempre in me.